A 9.4 Tesla Transmit and Receive MRI Quadrature Birdcage Coil Design and Fabrication for Mouse imaging

by

Ziyuan Fu

A thesis submitted to the Graduate Faculty of
Auburn University
in partial fulfillment of the requirements for the Degree of
Master of Science

Auburn, Alabama
December 13, 2014

Keywords: MRI, RF Coil, Quadrature, T/R Switch, Quadrature Hybrid, Low Noise Amplifier

Approved by

Shumin Wang, Chair, Associate Professor of Electrical and Computer Engineering
Stuart Wentworth, Associate Professor of Electrical and Computer Engineering
Lloyd Stephen Riggs, Professor of Electrical and Computer Engineering

Abstract

Magnetic Resonance Imaging (MRI) is an image modality used for clinical diagnosis as well as animal research. The study described in this thesis is intended for animal MRI application. In order to acquire high-resolution MRI images, radio-frequency (RF) coils are necessary in the experiments. In this study, we designed and fabricated a 9.4 Tesla high-pass transmit and receive birdcage coil for fMRI mouse imaging. The function of this system is to transmit RF energy to the subject generating a homogeneous volume B1+ field and then receive the RF energy with a pretty high SNR. The coil was designed by applying software simulations at first. Taken care of tuning, matching and other practical issues, the hardware implementation was done. Meanwhile, the front end for this system which includes T/R switch, Quadrature Hybrid, and LNA is discussed. By the end, MRI images of a saline water phantom acquired with the fabricated coil in a 9.4 Tesla MRI scanner demonstrate a high-level of excitation homogeneity and SNR, which correspond very well to the theory and simulation results.

Acknowledgments

First, I would like to thank Dr. Wang for giving me a great opportunity to learn and work in this lab and teaching me patiently for two and a half years. Also, I would like to thank Dr. Wentworth and Dr. Riggs for their courses I learnt and advice on this thesis. At the same time, I would like to thank my parents for their selfless love and support. At last, I would like to thank all the colleagues in our group: Hai Lu, Xiaotong Sun, Yu Shao, Shuo Shang, for their assistance on my research and all the people who have helped me in some way.

Table of Contents

List of Tables

List of Figures

List of Abbreviations

MRI	Magnetic Resonance Imaging
fMRI	functional Magnetic Resonance Imaging
RF	Radio Frequency
SNR	Signal to Noise Ratio
TX	Transmit
RX	Receive
PIN	Positive-Intrinsic-Negative
LNA	Low Noise Amplifier
UAB	University of Alabama at Birmingham

Chapter 1 MRI Basics

A basic knowledge of Magnetic Resonance Imaging (MRI) theory is very necessary in order to understand the intricacies of RF coil design and fabrication for functional MRI imaging.

In this chapter a brief introduction is given to the Physical Principles of nuclear Resonance. The MRI (Magnetic resonance Image) is based on the physical principles of nuclear magnetic resonance (NMR), which describe the behavior of certain nuclei in an applied magnetic field. The description below is based on a classical mechanical model, although NMR can be more accurately treated by quantum mechanics. Also, we will talk about some other issues, like MR signal detection, the free induction decay signal (FID), relaxation, coding in the rest part.

The next pages are divided in: the basics of MRI, the birdcage coil design and simulation, Front End design and fabrication, coil fabrication and scanner results, and future work.

1.1 Nuclear Spin and Properties

Some atomic nuclei has a property known as spin (angular momentum), which is the base of the NMR. The spin can be considered as an outcome of rotational or spinning motion of nucleus about its own axis. For this reason, nuclei having spin angular momentum are often referred to as nuclear spin. The spin angular momentum of a nucleus is defined by the spin quantum number p.

$$|P| = \frac{h}{2\pi}\sqrt{I(I+1)}$$

Where h is Planck's constant 6.626 × 10−34. The value of spin quantum number depends on the structure of nucleus (the number of protons and neutrons).

The human body mainly consists of water, H_2O, a molecule that contains two hydrogen atoms and an oxygen atom. A hydrogen atom consists of a nucleus containing one proton with an electron orbiting the nucleus. Quantum mechanical (QM) theory states that the proton rotates (or spins) around its own axis, and this phenomenon can be simply referred to as spin. The principles of MRI rely on the spinning motion of specific nuclei present in biological tissues. These are known as MR active nuclei. MR active nuclei are characterized by their tendency to align their axis of rotation to an applied external magnetic field. According to the laws of electromagnetic induction, nuclei that have a net charge and are spinning acquire a magnetic moment and are able to align with an external magnetic field. This occurs if the mass number is odd. The process of this interaction is angular momentum or spin.

Imagine a proton like a small sphere of distributed positive charge that rotates at a high speed about its axis, and this rotation produces an angular momentum. Moreover, particles associated with their orbital motion have an angular momentum. Then, consider the proton like a small sphere with a distributed charge appear some net charge circulating about its axis. Thus, this current produces a small magnetic field. Neutrons can also be thought of as a sphere of distributed positive and negative charges. But these charges are not uniformly distributed, for this reason, the neutron also generates a magnetic field when it spins. These small magnetic fields are called "magnetic moments". Here we symbolize it by μ. The relationship between the angular momentum J and the magnetic moment μ of a nucleus is given by:

$$\mu = \gamma \cdot p$$

Where γ is called gyromagnetic ratio. It is a characteristic of a particular nucleus and it is proportional to the charge-to-mass ratio of nucleus. Table 1 shows some relationships.

Table 1 Nuclear Spin and Gyromagneitc Ratio of some Nucleus

NMR Properties of some common Nuclei		
Nucleus	Nuclear Spin	Gyromagentic Ratio (MHz/T)
1H	1/2	42.58
13C	1/2	10.71
19F	1/2	40.05
23Na	3/2	11.26
31P	1/2	17.23

1.2 Behavior of Nuclei in an External Magnetic Field

In the absence of an applied external magnetic field all the nuclei of the material are oriented in random directions. When an external uniform magnetic field (B_0) influences to a group of protons, the interaction between the magnetic moment μ and the field B_0 tries to align the two.

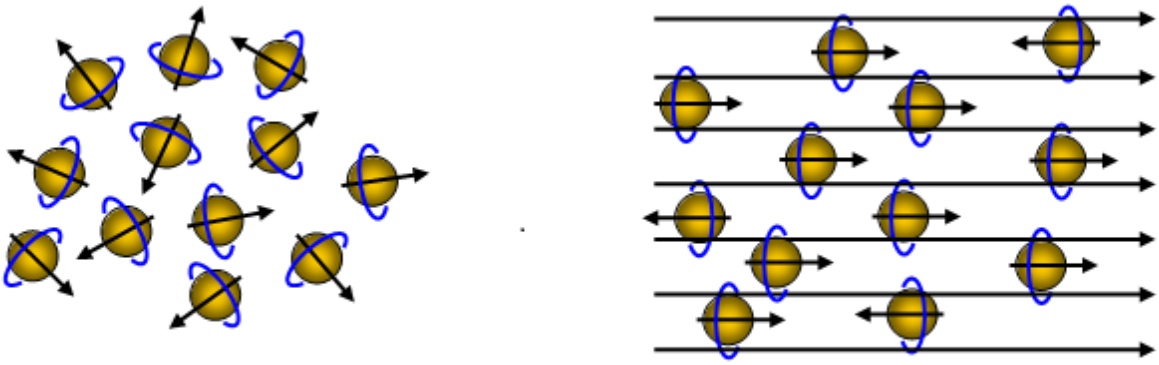

Figure 1.1 nuclei behavior when affected by an external magnetic field (B_0) and when not

To understand how particles with spin behave in a magnetic field, consider a proton. This proton has the property called spin. Think of the spin of this proton as a magnetic moment vector, causing the proton to behave like a tiny magnet with a north and a south pole. When the proton is placed in an external magnetic field, the spin vector of the particle aligns itself with the external field, just like a magnet would. There is a low energy configuration or state where the poles are aligned and a high energy state.

This particle can undergo a transition between the two energy states by the absorption of a photon. A particle in the lower energy state absorbs a photon and ends up in the upper energy state. The energy of this photon must exactly match the energy difference between the two states.

The difference in energy (ΔE) between the two states is proportional to the strength of the magnetic field B_0 and it is given by the expression:

$$\Delta E = \gamma B_0$$

The value of the precessional frequency is governed by the Larmor equation. The Larmor equation states that the processional frequency$\omega_0 = B_0 \times \gamma$, where $B_0$is the main magnetic field strength and γ is the gyro-magnetic ratio.

The gyro-magnetic ratio expresses the relationship between the angular momentum and the magnetic moment of each MR active nucleus. It is constant and is expressed as the precessional frequency of a specificMR active nucleus at 1 T. The unit of the gyro-magnetic ratio is therefore MHz/T. The gyro-magnetic ratio of hydrogen is 42.57 MHz/T. Other MR active nuclei have different gyro-magnetic ratios, and therefore have different precessional frequencies at the same field strength. In addition, different nuclei have different precessional frequencies at different field strengths. The precessional frequency is often called the Larmor frequency, because it is determined by the Larmor equation. As the gyro-magnetic ratio is a constant of proportionality, it is proportional to the Larmor frequency. Therefore if increases, the Larmor frequency increases.

1.3 The MR Signal

1.3.1 RF Pulse Excitation

Considering the large number of protons the magnetization vector is defined as the sum of all individual magnetic moments. The magnetization vector (M) is the one-to-one correspondence between the proton magnetic moment and its spin states; M is referred as the spin density of the system. This magnetization vector M in equilibrium precesses around the

external magnetic field. Therefore, M would only have a longitudinal component and it will not produce a detectable signal.

It is necessary perturb the signal from its equilibrium state and get M to precesses around B_0. This is done by applying a radiofrequency (RF) pulse that precisely meets the Larmor frequency of the nuclei of interest. This RF pulse generates a second magnetic field called B_1. Thus, B_1 is perpendicular to B_0 and rotates aboutB_0. The B_1 field is applied over the xy axis and its strength depends on the power transmitted per time value. The RF field B_1 is added at the Larmor frequency and it breaks the equilibrium of the tissue net spin, as a result, the magnetization is tipped away from the z direction at an angle of certain degree. The magnetization will rotate about the z direction at the Larmor frequency and hence spirals away from the longitudinal direction, towards the transverse plane. Eventually it can comes back to the equilibrium state (this phenomenon is called relaxation). This is because the applied radiofrequency corresponds to a photon energy that exactly equals the energy needed to cause the hydrogen dipole to flip from pointing along B_0 (high energy state) to pointing opposite B_0(low energy state).

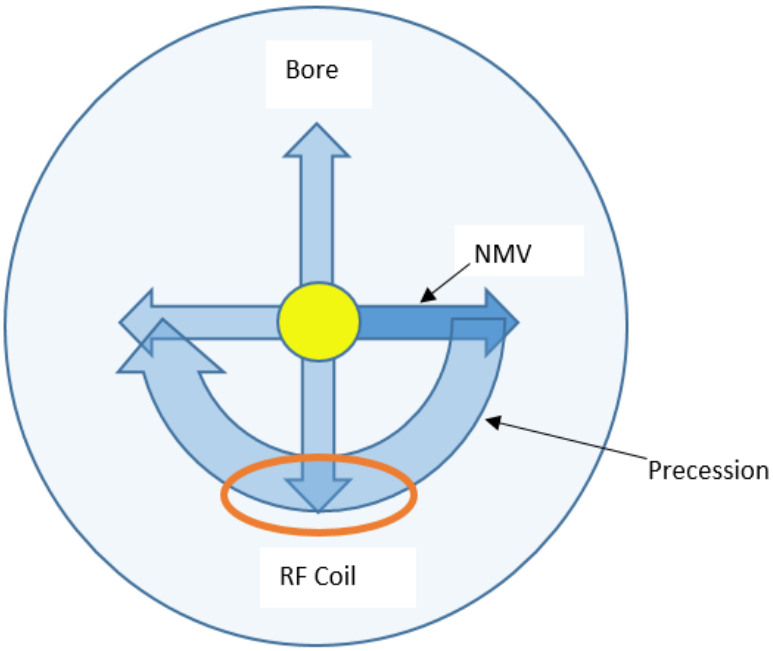

Figure 1.2 Generation of MR signal

1.3.2 The Free Induction Decay Signal (FID)

When the RF pulse is switched off, the NMV is influenced by B_0 field again and tries to realign with it. As a result, the hydrogen nuclei must lose the energy given to them by the RF pulse. The process by which hydrogen loses this energy is called relaxation. Because some of the high-energy nuclei return to the low-energy population, the NMV returns to realign with B_0 and align their magnetic moments in the spin-up direction. During relaxation hydrogen nuclei give up absorbed RF energy and the NMV returns to B_0. Independently, at the same time, the magnetic moments of hydrogen lose coherency because of dephasing. There are two terms we

need to care about. T1 recovery, the recovery of longitudinal magnetization caused by a process. And T2 decay, the decay of transverse magnetization caused by a process.

T1 recovery is caused by the nuclei giving up their energy to the surrounding environment or lattice, and it is termed spin lattice relaxation. Energy which is released to the surrounding lattice causes the magnetic moments of nuclei to recover their longitudinal magnetization. The rate of recovery is and exponential process. And a recovery time constant is called the T1 relaxation time, which takes 63% of the longitudinal magnetization to recover in the tissue. T2 decay is caused by the magnetic fields of neighboring nuclei interacting with each other. That is termed spin-spin relaxation, which results in decay or loss of coherent transverse magnetization. Also, the rate of decay is an exponential process, and the T2 relaxation time of a tissue is the time constant of decay. It takes 63% of the transverse magnetization to be lost while 37% remains. (Figure 1.3 and Figure 1.4)

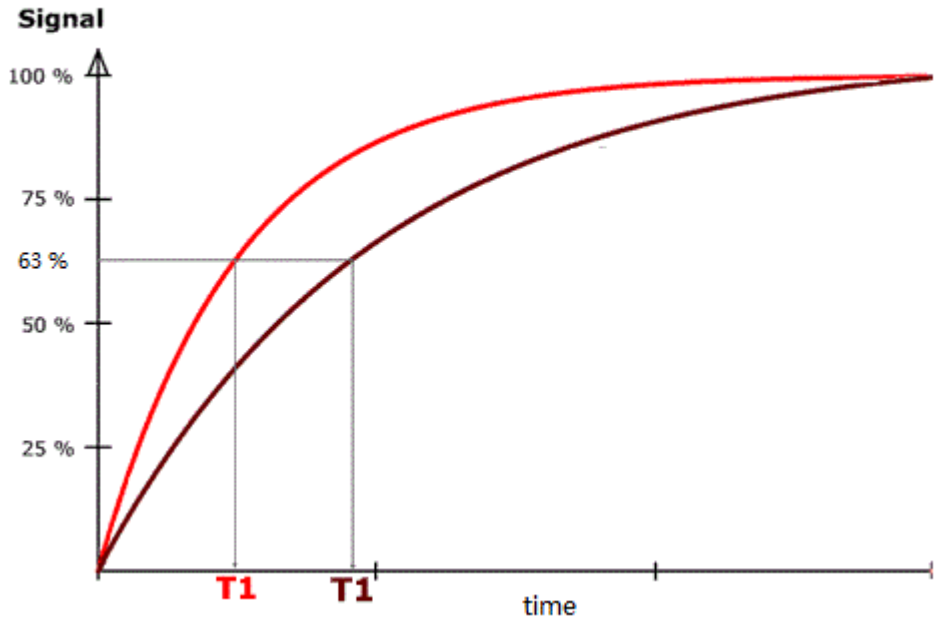

Figure 1.3 The T1 recovery curve of two tissues

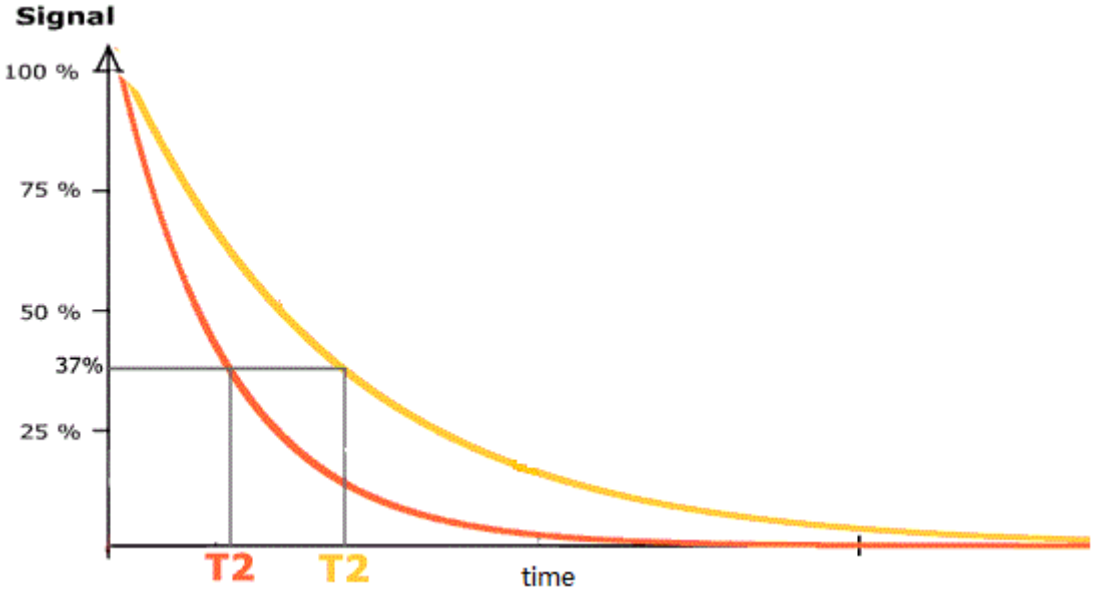

Figure 1.4 The T2 decay curve of two tissues

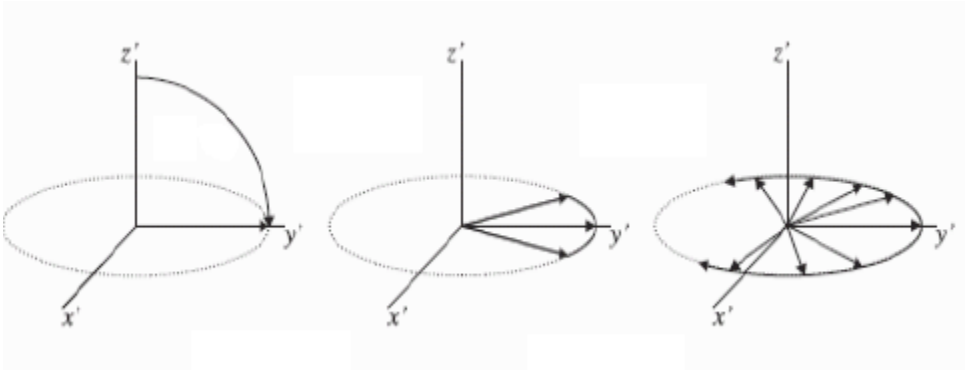

Figure 1.5 Dephasing

1.4 Magnetic Field Gradients

If each of the regions of spin was to experience a unique magnetic field we would be able to image their positions. A gradient in the magnetic field is what will allow us to accomplish this. A magnetic field gradient is a variation in the magnetic field with respect to position. A one-dimensional magnetic field gradient is a variation with respect to one direction, while a two-dimensional gradient is a variation with respect to two. The most useful type of gradient in magnetic resonance imaging is a one- dimensional linear magnetic field gradient. A one-dimensional magnetic field gradient along the x axis in a magnetic field,B_0 , indicating that the magnetic field is increasing in the x direction.

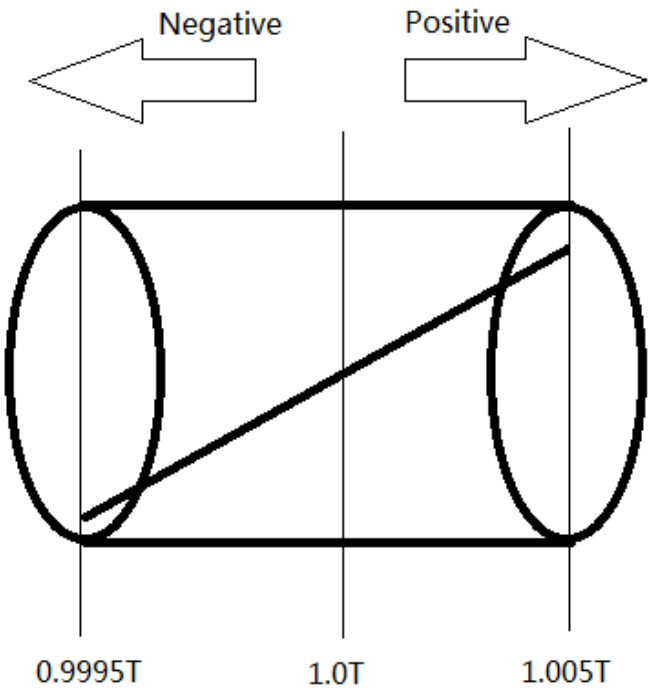

Figure 1.6 Gradients and change of field strength

1.4.1 Slice Selection

When a gradient coil is switched on, the magnetic field strength, and therefore the precessional frequency of nuclei located along its axis, is altered in a linear fashion. So, a specific point along the axis of the gradient has a specific precessional frequency. Therefore a slice situated at a certain point along the axis of the gradient has a particular precessional frequency. By transmitting RF energy with a band of frequencies coinciding with the Larmor frequencies within a particular slice as defined by the slice select gradient, a slice can therefore be selectively excited. Resonance of nuclei within the slice occurs because RF energy with the

same frequency is transmitted. A 90 Degree pulse contains a band of frequencies. This can be seen by employing the convolution theorem. The frequency content of a square 90 Degree pulse is shaped as a sinc pulse. The animation window displays the real components of this pulse. The amplitude of the sinc function is largest at the frequency of the RF which was turned on and off. This frequency will be rotated by 90 Degree while other smaller and greater frequencies will be rotated by lesser angles.

1.4.2 Frequency Encoding

Frequency encoding consists in add a gradient field along an arbitrary line "r" in the space, with this, it is possible to establish a relationship between spatial information along r and the frequencies of the MR signal. In this case, the Larmor frequency at r is:

$$\omega(\mathrm{r}) = \omega_0 = \gamma G_{Freq} r$$

$G_{Freq}\left(G_x, G_y, G_z\right)$ is the frequency-encoding gradient.

When a slice has been selected, the signal coming from it must be located align with both axes of the image. The signal is usually located along the long axis of the anatomy by a process called as frequency encoding. When the frequency encoding gradient is switched on, the magnetic field strength and therefore the precessional frequency of signal along the axis of the gradient, is altered in a linear fashion. The gradient therefore produces a frequency difference along its axis. The signal can now be located along the axis of the gradient according to its frequency.

1.4.3 Phase Encoding

Signal must now be located along the remaining axis of the image and this localization of signal is called phase encoding. When the phase encoding gradient is switched on, the magnetic field strength and therefore the precessional frequency of nuclei along the axis of the gradient is altered. When the speed of precession of the nuclei changes, the accumulated phase of the magnetic moments changes along the precessional path. Nuclei which have sped up because of the presence of the gradient move further around their precessional path than if the gradient had not been applied while nuclei that have allowed down due to presence of the gradient move further back .There is now a phase difference between nuclei positioned along the axis of the gradient. When the phase encoding gradient is switched off, the magnetic field strength experienced by the nuclei returns to the main field strength, therefore the precessional frequency of all the nuclei returns to the Larmor frequency. The nuclei travel at the same speed around their precessional paths, however, their phases or positions on the clock are different. This difference in phase between the nuclei is used to determine their position along the phase encoding gradient.

1.5 Summary

It is necessary to understand the basic principles of MRI in order to design and fabricate coils. When a patient or sample is inserted into the MRI scanner, the NMV will be aligned in the direction of the main magnetic field. The role of the transmit coil is to tip tis magnetization to the transversal plane. The magnetization will rotate transversally, and the flux from the magnetization induces a voltage in the receive coil. The geometric positioning with respect to the precessing magnetization is important in order to receive as much flux as possible. When

the magnetization is restored to its equilibrium direction along the main magnetic field, no signal is induced in the coil. Also, the content above introduced the basic mechanisms of gradients, how signals are determined in all three dimensions and how data is acquired.

Chapter 2 Theory and Design of the Birdcage Coil

RF coils are the receivers, transmitters, or sometimes transceivers of radiofrequency signals in the magnetic resonance imaging (MRI) hardware. The MR signal in MRI, is produced by the process of resonance, which is the result of radiofrequency coils. They consist of two electromagnetic coils, the transmitter generating electromagnetic fields, and receiver coils receiving electromagnetic fields.

We can classify RF coils based on the functions, structures and other factors. Such as transmit receive coil, receive only coil, and transmit only coil based on the functions, or surface coil, volume coil, phase array coil, solenoid coil, quadrature coil, Hekmholtz's coil based on the structures. For this RF coil, it is transmit and receive quadrature birdcage coil. Specifically, the birdcage coil generates RF pulses at the Larmor frequency (400Mhz) to excite the nuclei in the subject to be imaged. When the TX pulse is turned off the nuclei will relax. The nuclei will emit RF energy at Larmor frequency (400Mhz) during relaxation. At the same time the birdcage coil will work as a receive coil and that energy will be received.

In the following discussions, we will talk about the theory, modeling and simulation of this quadrature birdcage coil.

2.1 Introduction

Birdcage coils are widely used in magnetic resonance imaging (MRI) applications for their ability to operate in transmit/receive mode with wide homogeneous field and high signal-to-noise ratio.

The first cylindrical birdcage coil was designed and fabricated by Hayes, which was a high pass coil producing a linearly polarized field. At the same time, a quadrature coil produces a circularly polarized field and is preferred over a linear coil since it improves the SNR by a factor of$\sqrt{2}$, and reduces RF transmit power. Specifically, the SNR increases because the noise voltage generated in the two orthogonal modes are not correlated but the signals from the nuclei are correlated. For a quadrature coil, we need to drive it at two ports by using the equal amplitude and 90 degree phase difference.

In the design of a RF coil, a RF shield is very necessary. Basically, it performs two functions. First, it reduces the interaction between the RF coil and the gradient or the shim coils. Second, it improves the transmit efficiency by preventing the radiation of the coil. At the same time, it provides a stable environment for tuning and matching. At high fields the radiation losses are very high. And it is necessary to make the shield cover the coil completely. Generally, the diameter of the shield should be 1.5 times the diameter of the coil and the length the coil should be about 60% that of the shield.

2.2 Theory of Birdcage Coil

The birdcage coil is a volume coil. Volume coils are preferred over surface coils in some aspects. A very important point is that volume coils have a bigger field of view compared to surface coils and thus volume coils can produce a homogenous B1 field in the volume of interest so that the nuclei can be uniformly excited and a homogenous image can be obtained.

The birdcage coils physically consist of multiple parallel conductivity segments equally spaced that are parallel to z axis. These parallel conductive segments are called legs or rungs.

And two circular end rings to denote the end loop. For a high-pass birdcage coil, the conductive loops have capacitors between adjacent rungs (inductor). A low-pass coil is where the capacitors at the mid-point of the rungs; the conductive loop in this case are inductors. And a hybrid coil is where the capacitors are located on the loop segments and the rungs. Capacitors are situated at the center of rung because the voltage at the center of rungs is zero. A so called high-pass is as the high frequency signals will tend to pass through capacitive elements in the conductive loops because at high frequency the capacitors will present low impedance compared to inductors, which will give high impedance. Conversely, low frequency signals will be blocked by capacitive elements that will give high impedance and shorted by inductive elements as they will give low impedance.

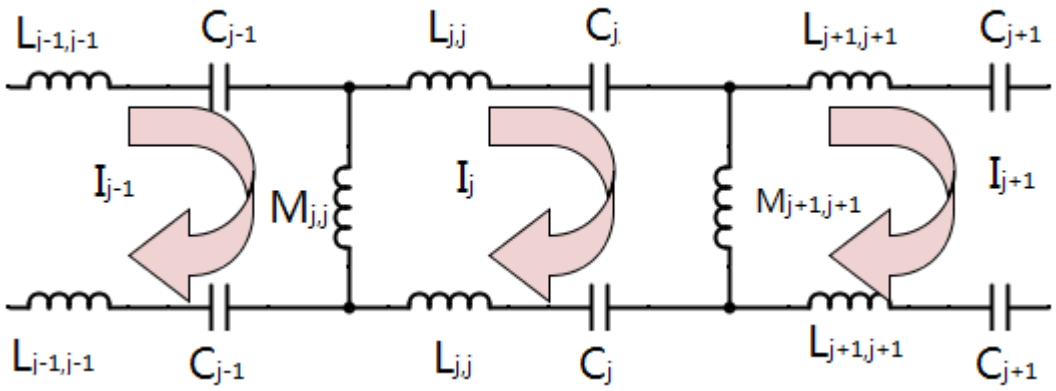

Figure 2.1 Equivalent circuit for a high-pass Birdcage Coil

The meshes repeats N times, where N is the number of legs. The end ring segments of the two conducting loops are represented by inductors and capacitors. The adjoining meshes to

the feed point ($I_{j+!,}I_{j-1}$) are mutually inductively coupled (M_{j+1},M_{j-1}) to the feed mesh. When the coil is fed at a particular location it creates N/2+1 resonant modes.

Applying Kirchhoff's voltage law to the schematic shown above, we get

$$-i\omega M(I_j - I_{j-1}) - i\omega M(I_j - I_{j+1}) - 2i\omega L I_j + \frac{2i}{\omega C} I_j = 0, j = 1,2, \ldots . N$$

From the equation above, we can get

$$M(I_{j+1} + I_{j-1}) + 2(\frac{1}{\omega^2 C} - L - M)\, I_j = 0, j = 1,2, \ldots . N$$

As for this symmetrical structure, we can get

$$I_j = I_{j+N}$$

Therefore, the N independent solutions should have the form as following,

$(I_j)m = cos\frac{2\pi mj}{N}$; when m=0,1,2….,$\frac{N}{2}$

$(I_j)m = sin\frac{2\pi mj}{N}$; when m=0,1,2….,$\frac{N}{2}$-1

We can find the resonant frequencies and modes by substituting the equations back, the form should be as following:

$$\omega_m = [C\left(L + 2Msin^2\frac{\pi m}{N}\right)]^{-1/2} \qquad \text{m=0,1,2,….}\frac{N}{2}$$

In this equation: when m=1 we got the dominant mode; when m=0 we got the end-ring mode.

2.3 Simulation of Birdcage Coil

For designing for a coil, we should know the scanner system and accessories very well, including the dimensions, customer need and other details. And we can see the Figure 2.2 shows the ball, from which we determined the outer diameter of the coil is 114mm. Figure 2.3 shows the animal bed, from which we determined the inner diameter of the coil is 88mm. The coil is designed as a high-pass coil and the number of legs we chose here is 8.

Figure 2.2 Scanner Bore

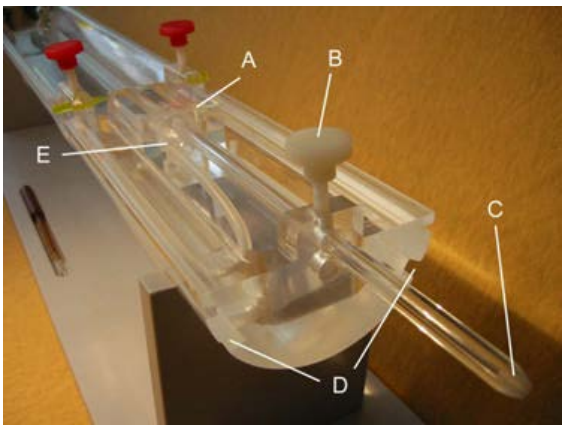

Figure 2.3 Animal Bed

Once the dimensions and shape were decided, we modeled and simulated the coil in software FEKO. We can see from the figures below, there are totally three parts, the shield, the

coil and the phantom. We set the material of shield to be copper. As we will use AWG#16 copper wire for the coil fabrication, we needed to set the wire to be copper with a diameter of 1.3mm. The dielectric modeling for the phantom should be, relative permittivity 78, conductivity 0.657S/m.

The main purposes for simulating the coil include: 1) Determine the values of capacitors. 2) Excite the coil and generate the B1+ field to make sure the design is good. Now we will discuss how to simulate the coil fast and precisely. The first step we did is to tune the coil to make the dominant mode be resonant at 400Mhz. As we all know the time we spend on simulation for one time is a very important evaluation for the simulation. And for this simulation, there are two dominant parameters determining the simulation time, mesh size and frequency sweep points. For the first step, we just needed to know nearly value of the capacitor to tune the dominant mode to 400Mhz. So we can set the mesh size bigger and the sweep points less. (Figure 2.4) Here I set the parameters as following: Triangle edge length 15mm, wire segment length 5mm, wire segment radius 0.05, frequency increment 2.7Mhz from 50Mhz to 450Mhz. After tuning the dominant mode to 400Mhz, we got the capacitor value 2.85PF. (Figure 2.5)

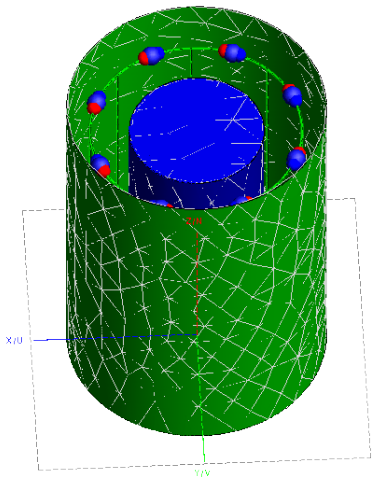

Figure 2.4 Coil Model with coarse mesh

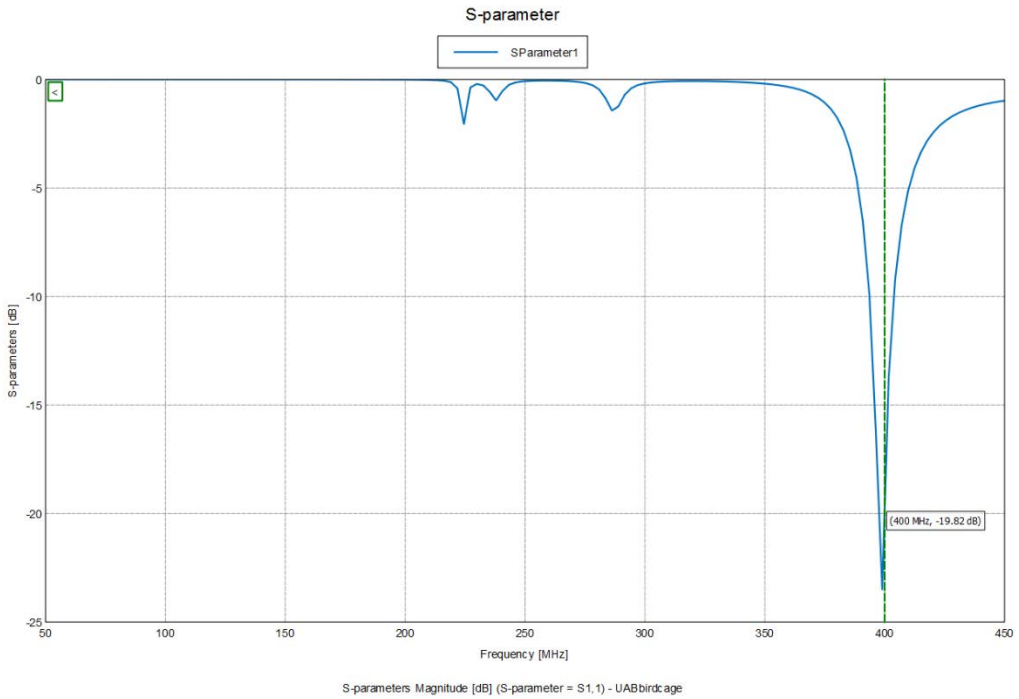

Figure 2.5 S11 of one excitation port from 50Mhz to 450Mhz

The second step is to determine the capacitor value precisely to be a reference for purchasing components. So I set the mesh size much smaller and frequency increment smaller in a much smaller span, for we have got a nearly value to start with. So here are the parameters: Triangle edge length 8mm, wire segment length 2mm, wire segment radius 0.01, frequency increment 416.7khz from 395Mhz to 405Mhz. After tuning the dominant mode to 400Mhz, we got the capacitor value 2.78PF.

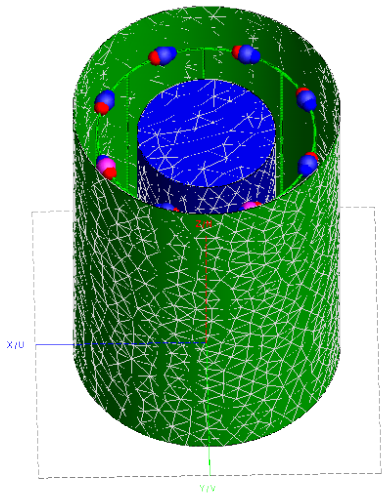

Figure 2.6 Coil Model with fine mesh

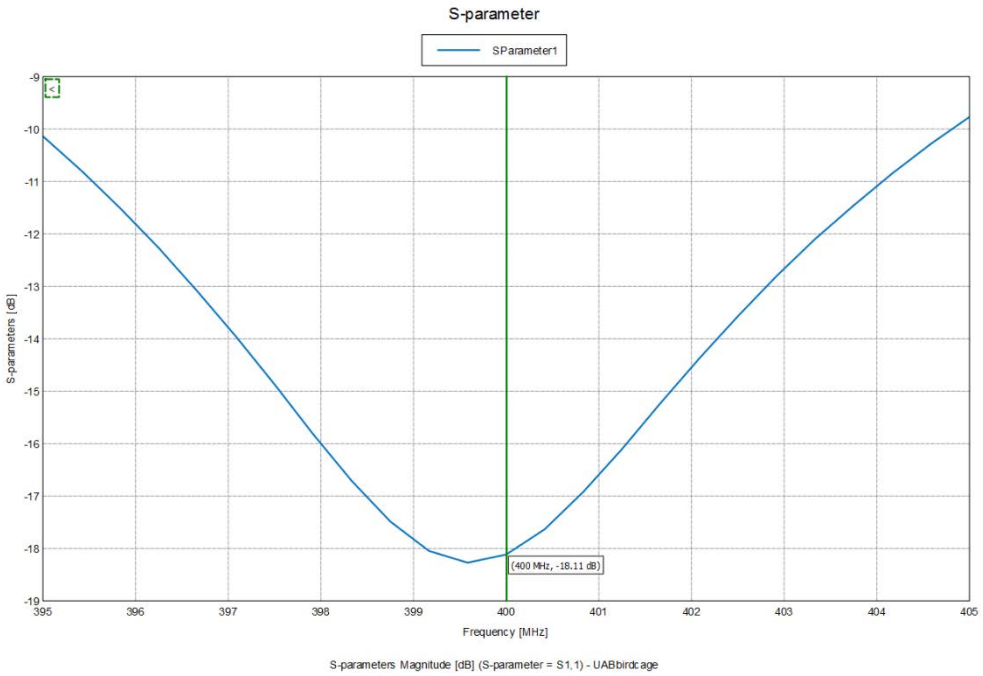

Figure 2.7 S11 of one excitation port from 50Mhz to 450Mhz

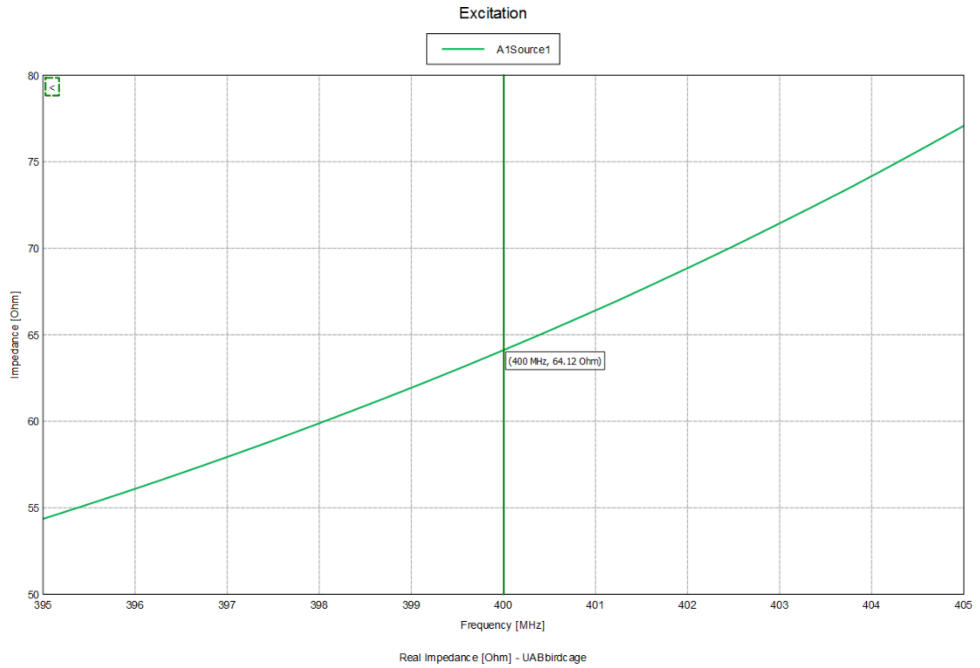

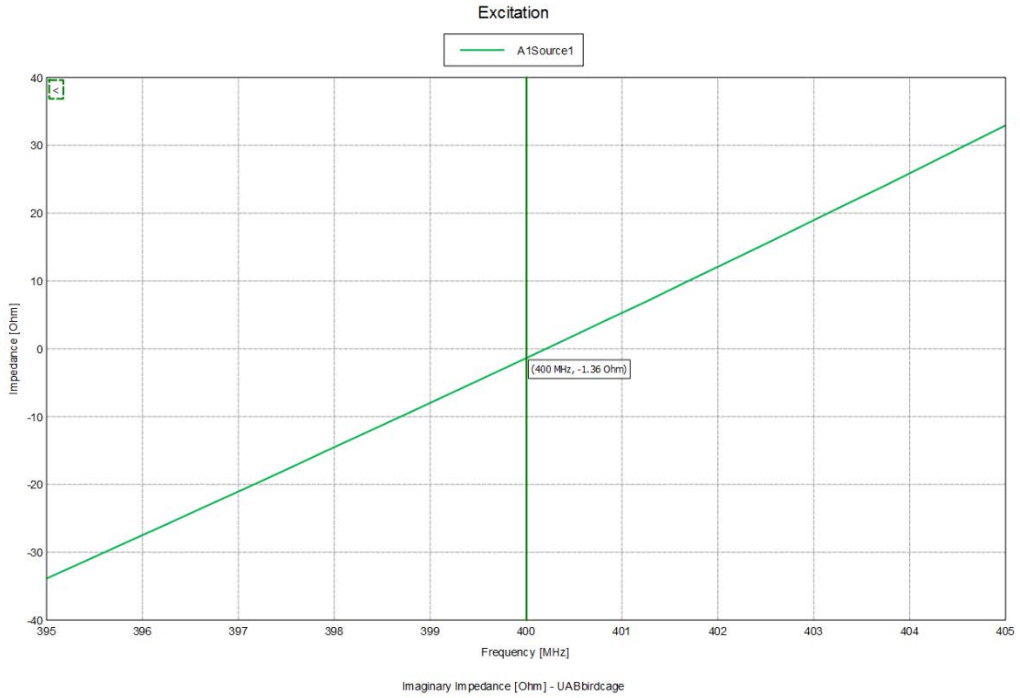

Figure 2.8 Real part and Imaginary part of the impedance of the Coil

So after we have got the capacitors we need to purchase for the fabrication. We come to the last step to excite the coil and generate B1 field. As the same as for real scanning, we need to simulate in three planes, transverse, sagittal and coronal. (Figure 2.9)

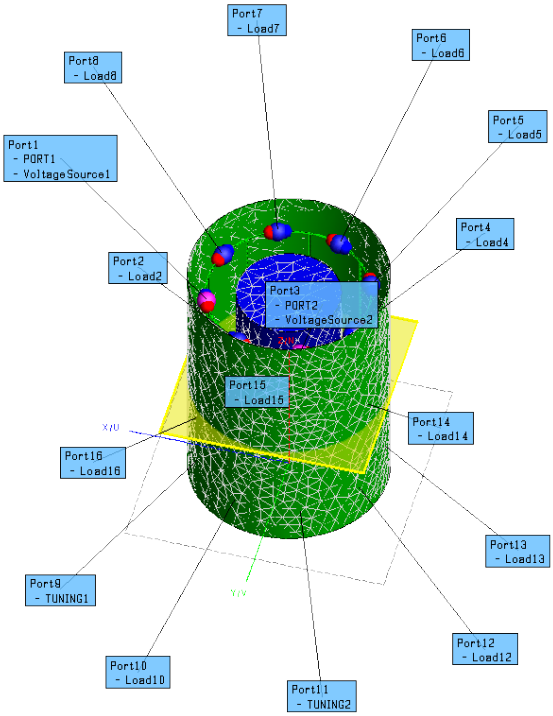
Port7
- Load7
Port8
- Load8
Port6
- Load6
Port5
- Load5
Port1
- PORT1
- VoltageSource1
Port4
- Load4
Port2
- Load2
Port3
- PORT2
- VoltageSource2
Port15
- Load15
Port14
- Load14
Port16
- Load16
Port13
- Load13
Port9
- TUNING1
Port12
- Load12
Port10
- Load10
Port11
- TUNING2

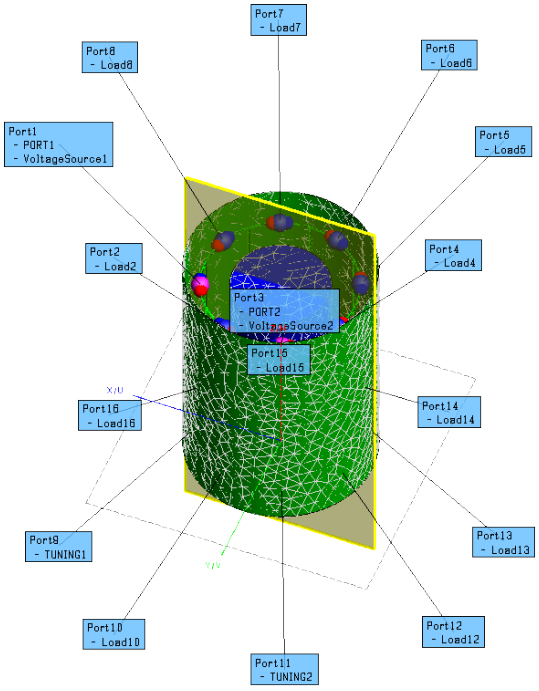
Port7
- Load7
Port8
- Load8
Port6
- Load6
Port1
- PORT1
- VoltageSource1
Port5
- Load5
Port2
- Load2
Port4
- Load4
Port3
- PORT2
- VoltageSource2
Port15
- Load15
Port16
- Load16
Port14
- Load14
Port9
- TUNING1
Port13
- Load13
Port10
- Load10
Port12
- Load12
Port11
- TUNING2

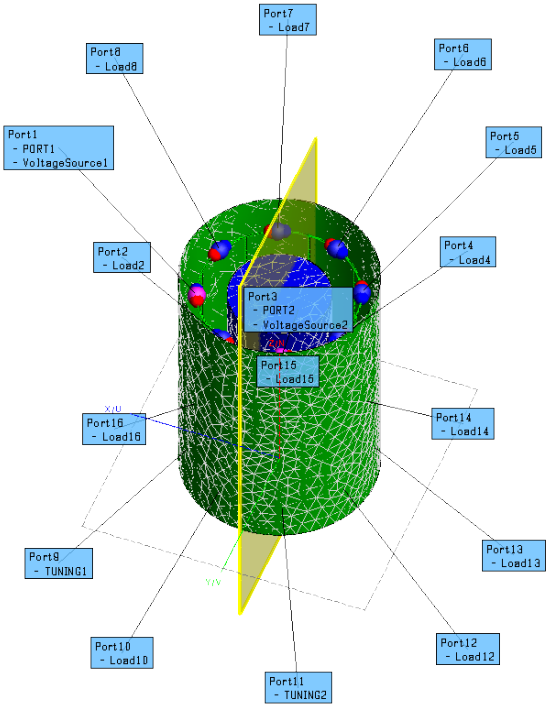

Figure 2.9 Different cutting planes. 1) Top: transverse plane. 2) Middle: sagittal plane. 3) Bottom: coronal plane.

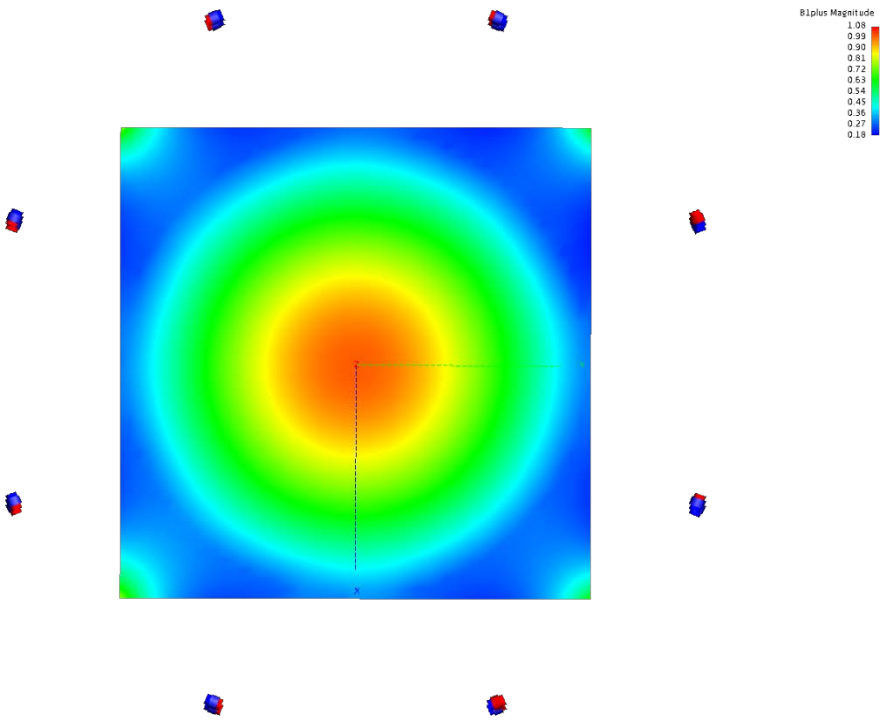
B1plus Magnitude
1.08
0.99
0.90
0.81
0.72
0.63
0.54
0.45
0.36
0.27
0.18

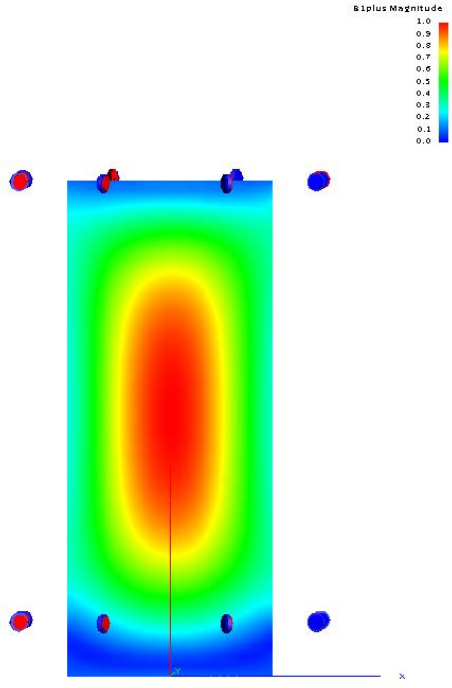
B1plus Magnitude
1.0
0.9
0.8
0.7
0.6
0.5
0.4
0.3
0.2
0.1
0.0

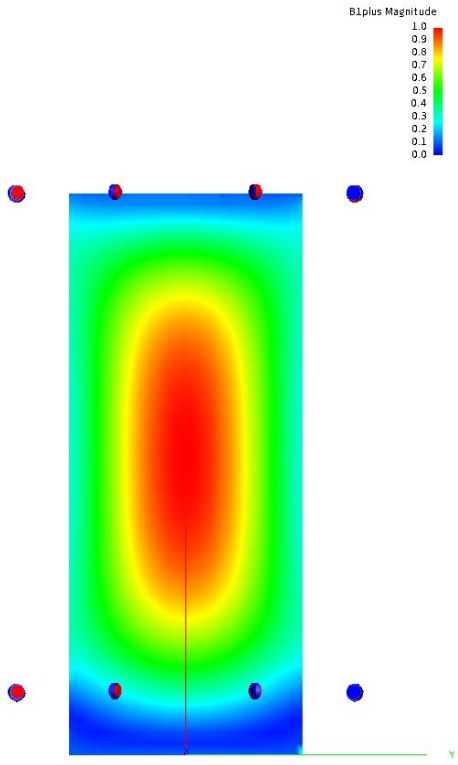

Figure 2.10 B1+ field distribution. 1) Top: transverse plane. 2) Middle: sagittal plane. 3) Bottom: coronal plane.

We can see the profile from Figure 2.10 corresponds to the theory very well, so the simulation is done.

Chapter 3 Front End Circuit Design

The RF front end is a generic term for all the circuitry between the coil and the scanner system. For this 9.4T transceiver birdcage, it consists of two Transmit-Receive switch (T/R switch), a Quadrature hybrid and a Low Noise Amplifier (LNA).

When the DC for the T/R switch is on, the transmit signal from the scanner system will go through to the Quadrature hybrid. Then the Quadrature hybrid will split the signal into two signals, equal magnitude and 90 degree phase difference. And these two signals will flow to the two exciting ports on the coil to make the coil generate magnetic field. When the signal from the subject is received to the coil, the two signals are combined by the Quadrature hybrid. And the combined signal will go through T/R switch when DC for the T/R switch is off to the LNA. After being amplified, the signal flow to the scanner system and processed by the background program.

That is how the front end circuit works. And the three components, Transmit-Receive switch (T/R switch), Quadrature hybrid, and Low Noise Amplifier (LNA), will be discussed in theory, design, simulation and bench test results in the following section.

3.1 T/R Switch

3.1.1 Introduction

Switch, as a control circuit, has been used extensively in radar, communication systems, electronic warfare, wireless applications, instruments, and other systems for controlling the

signal flow. In microwave systems, the transmitter and receiver section is called a transceiver. Transceivers have different requirements for switches including low and high power, narrowband and broadband, and high isolation. Lumped elements play an important role in achieving broad bandwidths, high isolation, and high power levels in RF/microwave switches.

For this front end circuit, we designed two T/R switch. One for Transmitting, connected the TX signal from the system to the Quadrature hybrid. One for Receiving, connected the Quadrature hybrid to the LNA.

3.1.2 Design and Simulation

The key points for this design are Lumped-element PI network, Lumped-element LC tank and PIN Diode control. As for the receive part. When receiving signal from the coil, DC signal is off and RF signal flows through the PI network to the RX port. And when DC signal is on, Diode current flow, which is in parallel with the PI network, forms a high impedance to block the two ports. In order to enhance the isolation, we design two PI networks in series. As for the transmit part. When transmitting signal to the coil, DC signal is on and RF signal flows through the Diode to the coil. And when DC signal is off, RF signal will flow to the LC tank to form the isolation between the TX port and the coil.

The Figure 3.1 below shows the schematic illustrating this design.

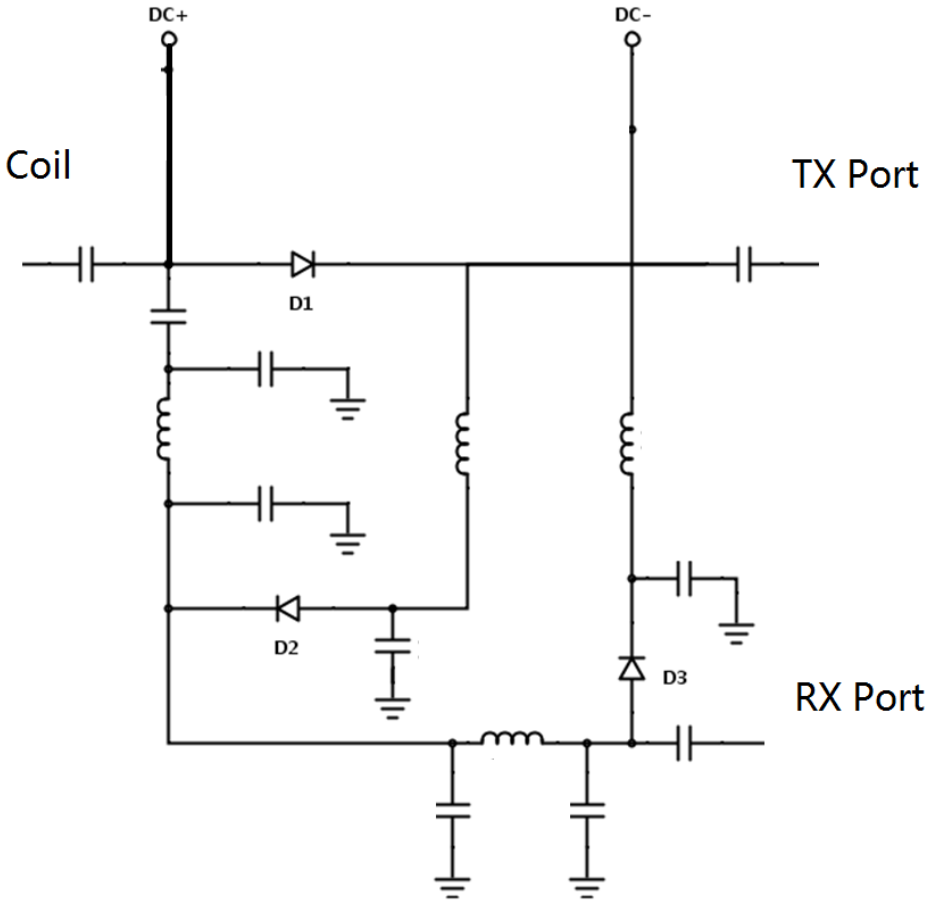

Figure 3.1 Schematic of T/R switch

We need to determine the components for the PI network, so we simulate it in the ADS. And we got the value of the capacitor is 2PF.

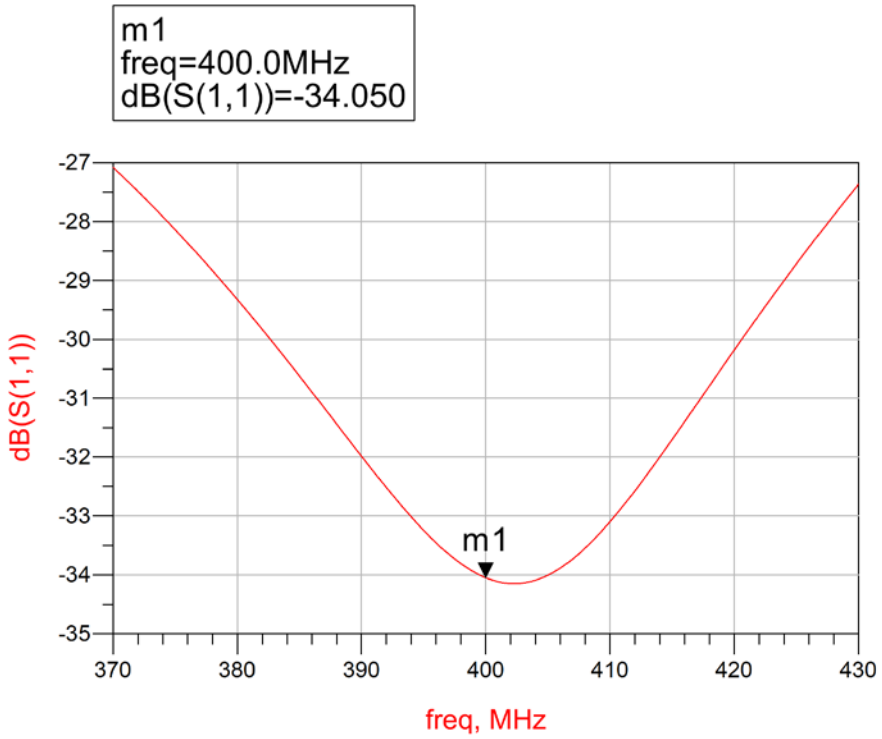

Figure 3.2 S11 of the two PI network in series

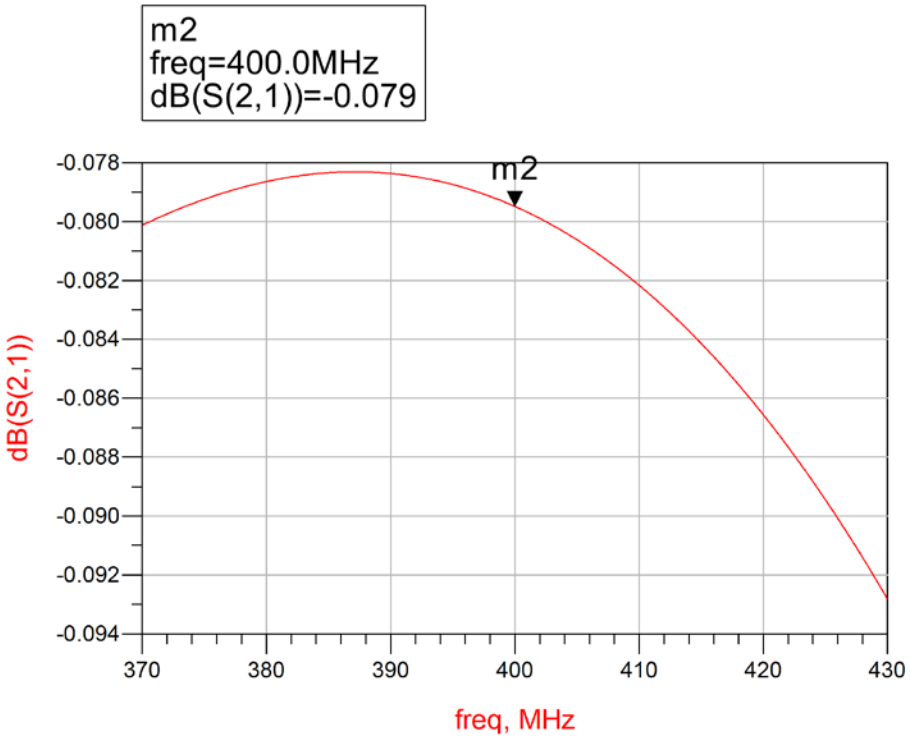

Figure 3.3 S21 of the two PI network in series

3.1.3 Bench Test Results

We fabricated T/R switch on the layout. After tuning the trimmer inductors, we can get the optimized results shown as following.

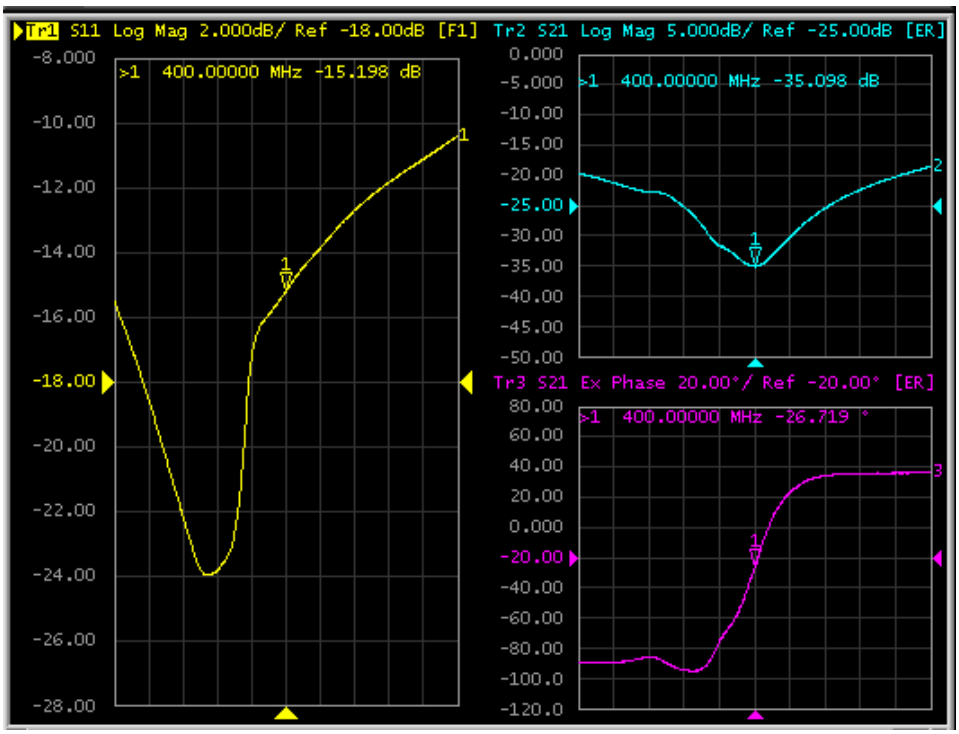

Figure 3.4 S11 and S21 for Coil Port to TX Port when DC is OFF

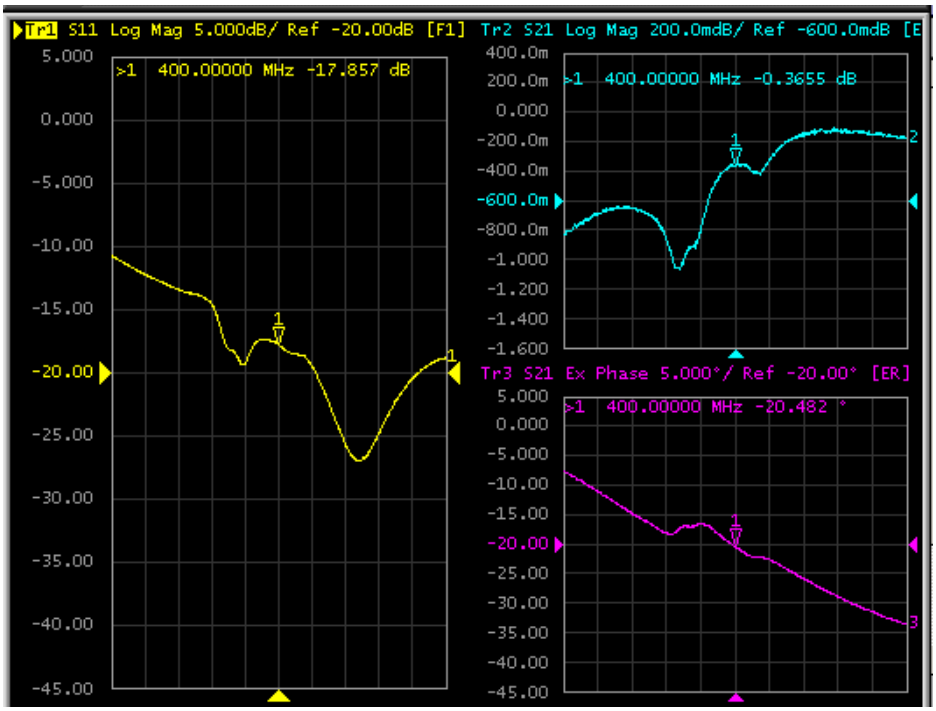

Figure 3.5 S11 and S21 for Coil Port to TX Port when DC is ON

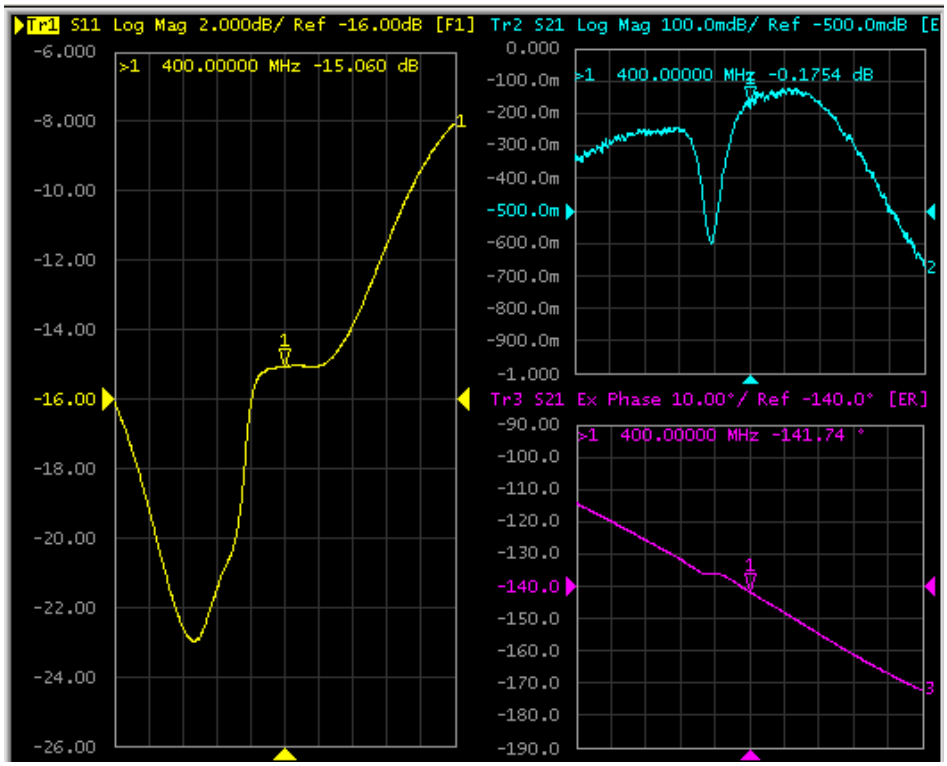

Figure 3.6 S11 and S21 for Coil Port to RX Port when DC is OFF

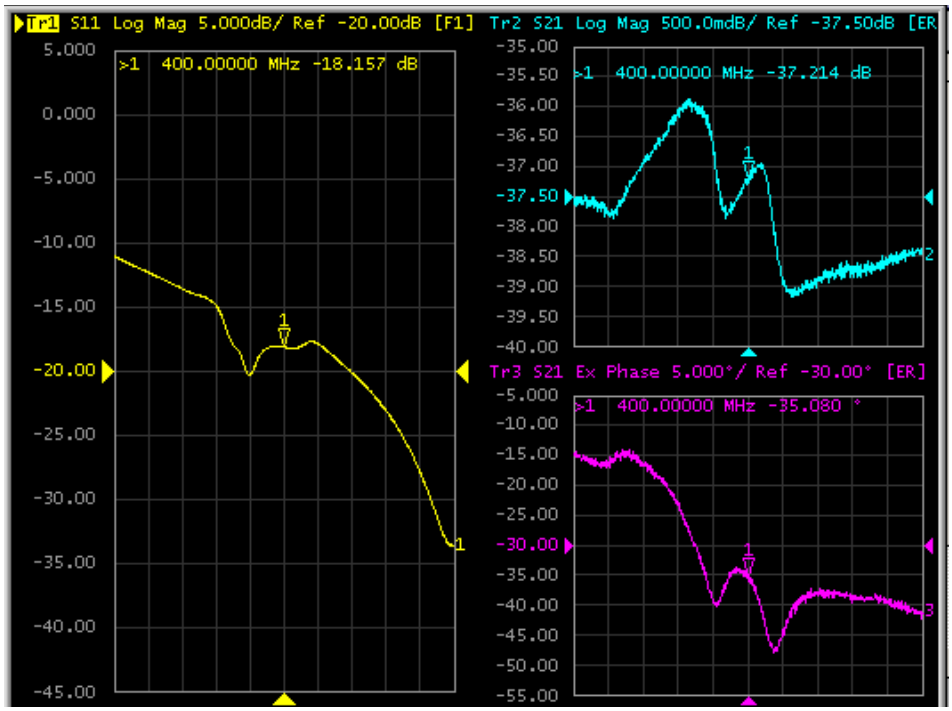

Figure 3.7 S11 and S21 for Coil Port to RX Port when DC is ON

We should be careful with the DC Pin Diode signal from the scanner system. As for this Bruker scanner system, the positive conduct voltage is 3.8V. And for this T/R switch design, we should apply at least 3.2V positive voltage to drive the Pin Diode to conduct completely. So, here we provided the DC signal to the two T/R switches in parallel. The total current is 242mA.

3.2 Quadrature Hybrid

3.2.1 Introduction

A hybrid coupler is a passive device used in RF circuits. And Quadrature hybrids are 3 dB directional couplers with a 90◦phase difference in the outputs of the through and coupled

arms. This type of hybrid is often made in microstrip line or stripline form and is known as a branch-line hybrid, too. Other 3 dB couplers, such as coupled line couplers or Lange couplers, can also be used as quadrature couplers.

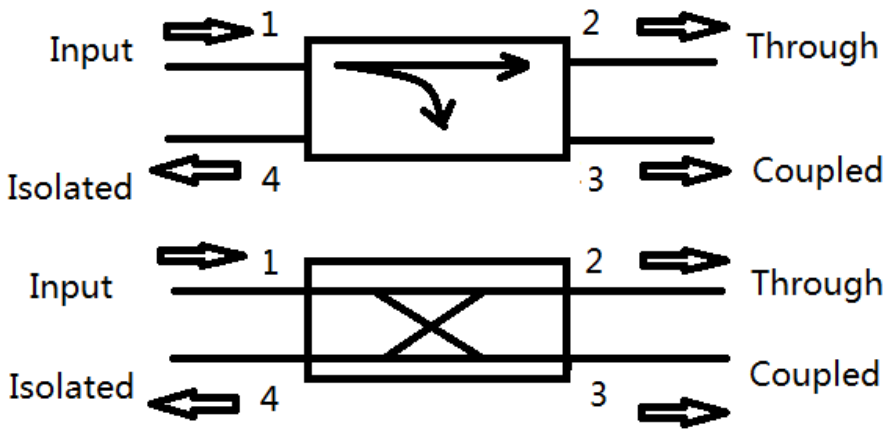

Figure 3.8 Two commonly used symbols for directional couplers

We analyze this device starting from a Four-Port Network or Directional Coupler. Consider a reciprocal four-port network matched at all ports, which should have the scattering matrix as the following form:

$$[S] = \begin{bmatrix} 0 & S_{12} & S_{13} & S_{14} \\ S_{12} & 0 & S_{23} & S_{24} \\ S_{13} & S_{23} & 0 & S_{34} \\ S_{14} & S_{24} & S_{34} & 0 \end{bmatrix}$$

If the network is lossless, equations result from the unitarity. Consider the multiplication of row 1 and row 2, and the multiplication of row 4 and row 3:

$$S_{13}^{*}S_{23} + S_{24}S_{14}^{*} = 0$$
$$S_{13}S_{14}^{*} + S_{23}S_{24}^{*} = 0$$

Simplification can be made by choosing the phase references on three of the four ports. So, we choose S12= S34 =α, S13 =$\beta e^{j\theta}$, and S24 =$\beta e^{j\theta}$, where α and β are real, and θ and $\emptyset$ are phase constants to be determined. We can get the equation.

$$S_{12}^{*}S_{13} + S_{34}S_{24}^{*} = 0$$

And this equation yields a relationship between the remaining phase constants as

$$\theta + \emptyset = \pi \pm 2n\pi$$

Ignore 2π, we can get two particular choices.

The first one is a symmetric coupler ($\theta = \emptyset = \pi/2$). Then the scattering matrix has the following form:

$$[S]=\begin{bmatrix} 0 & \alpha & j\beta & 0 \\ \alpha & 0 & 0 & j\beta \\ j\beta & 0 & 0 & \alpha \\ 0 & j\beta & \alpha & 0 \end{bmatrix}$$

The other one is an anti-symmetric coupler ($\theta = 0$,$\emptyset = \pi$). Then the scattering matrix has the following form:

$$[S]=\begin{bmatrix} 0 & \alpha & \beta & 0 \\ \alpha & 0 & 0 & -\beta \\ \beta & 0 & 0 & \alpha \\ 0 & -\beta & \alpha & 0 \end{bmatrix}$$

The basic operation of a directional coupler can be illustrated with Figure, which shows two commonly used symbols for a directional coupler and the port definitions. Power supplied to port 1 is coupled to port 3 (the coupled port), when the remainder of the input power is

delivered to port 2 (the through port) with the coefficient. For an ideal directional coupler, no power is delivered to port 4 (the isolated port).

The following quantities are commonly used to characterize a directional coupler:

$$\text{Coupling}=\text{C}=10\log\frac{\text{P}_1}{\text{P}_3}$$

$$\text{Directivity}=\text{D}=10\log\frac{\text{P}_3}{\text{P}_4}$$

$$\text{Isolation}=\text{I}=10\log\frac{\text{P}_1}{\text{P}_4}$$

$$\text{Insertion loss}=\text{L}=10\log\frac{\text{P}_1}{\text{P}_2}$$

The coupling factor indicates the fraction of the input power which is coupled to the output port. And the directivity is the coupler's ability to isolate forward and backward power. The isolation is a measure of the power delivered to the uncoupled port. The insertion loss means the input power delivered to the through port, diminished by power delivered to the coupled and isolated ports. The ideal coupler has infinite directivity and isolation (S_{14} = 0).

With reference to Figure 3.9, the basic operation of the branch-line coupler is as follows. With all ports matched, power entering port 1 is evenly divided between ports 2 and 3, with a 90◦phase shift between these outputs. No power is coupled to port 4 (the isolated port).

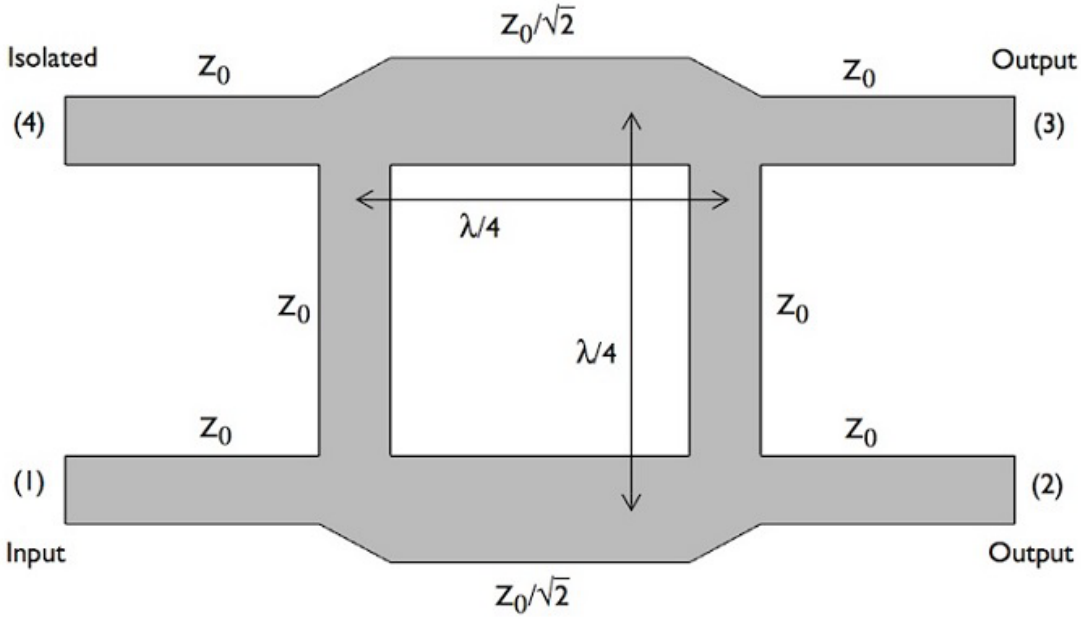

Figure 3.9 Geometry of a branch-line coupler

And the scattering matrix should be the form as following:

$$[S]=\frac{-1}{\sqrt{2}}\begin{bmatrix}0 & j & 1 & 0\\ j & 0 & 0 & 1\\ 1 & 0 & 0 & j\\ 0 & 1 & j & 0\end{bmatrix}$$

3.2.2 Design and Simulation

We used PI-network lumped-element components here. First we calculated the theory values applying the following equations:

$$C=\frac{1}{\sqrt{2}Z_0\omega} \qquad L=\frac{\sqrt{2}Z_0}{\omega}$$

For the Z_0 PI-network, $\sqrt{2}Z_0$=50Ohm, and for the $Z_0/\sqrt{2}$ PI-network, $\sqrt{2}Z_0$=50/$\sqrt{2}$Ohm.

After calculation of the theory values, we input the layout design into ADS and tuned the values of the capacitors and inductors to get the optimized results. For the Quadrature hybrid, the parameters we keep a watchful eye on S11 of the port1, S21 (magnitude and phase) of port2 and port3, and S41 (Isolation) of port4.

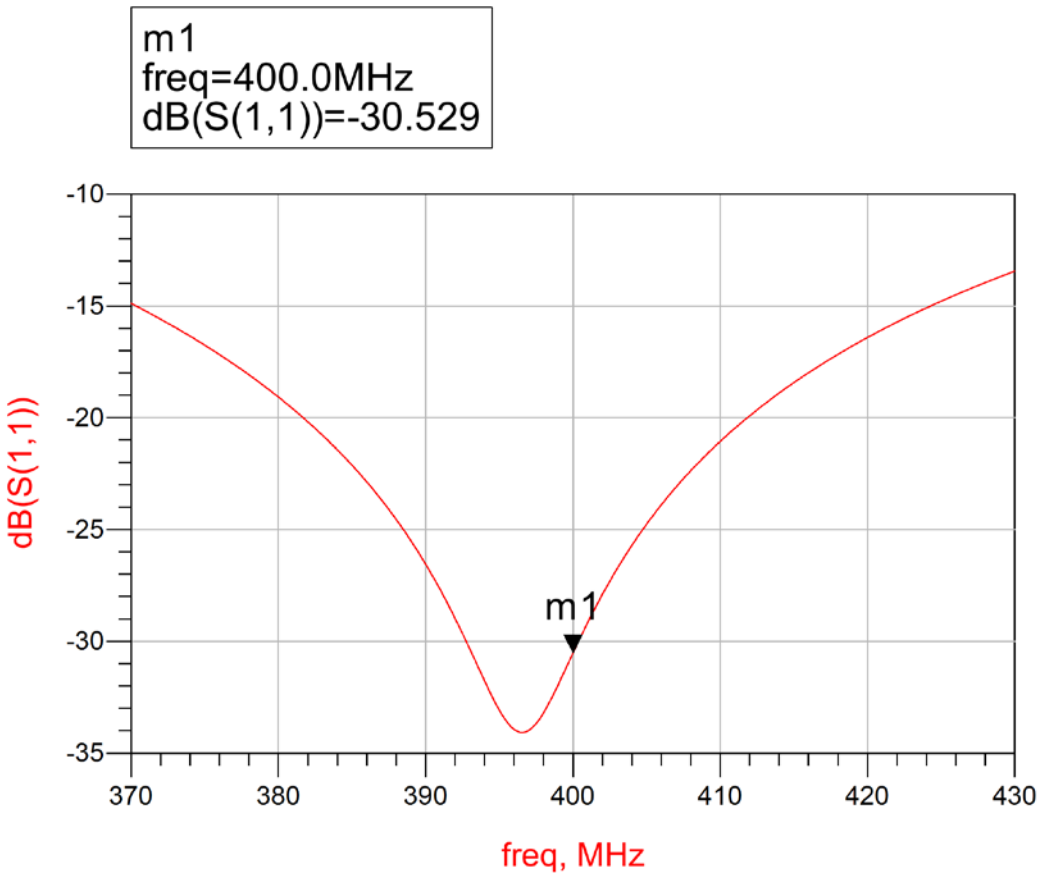

Figure 3.10 S11 of PORT1

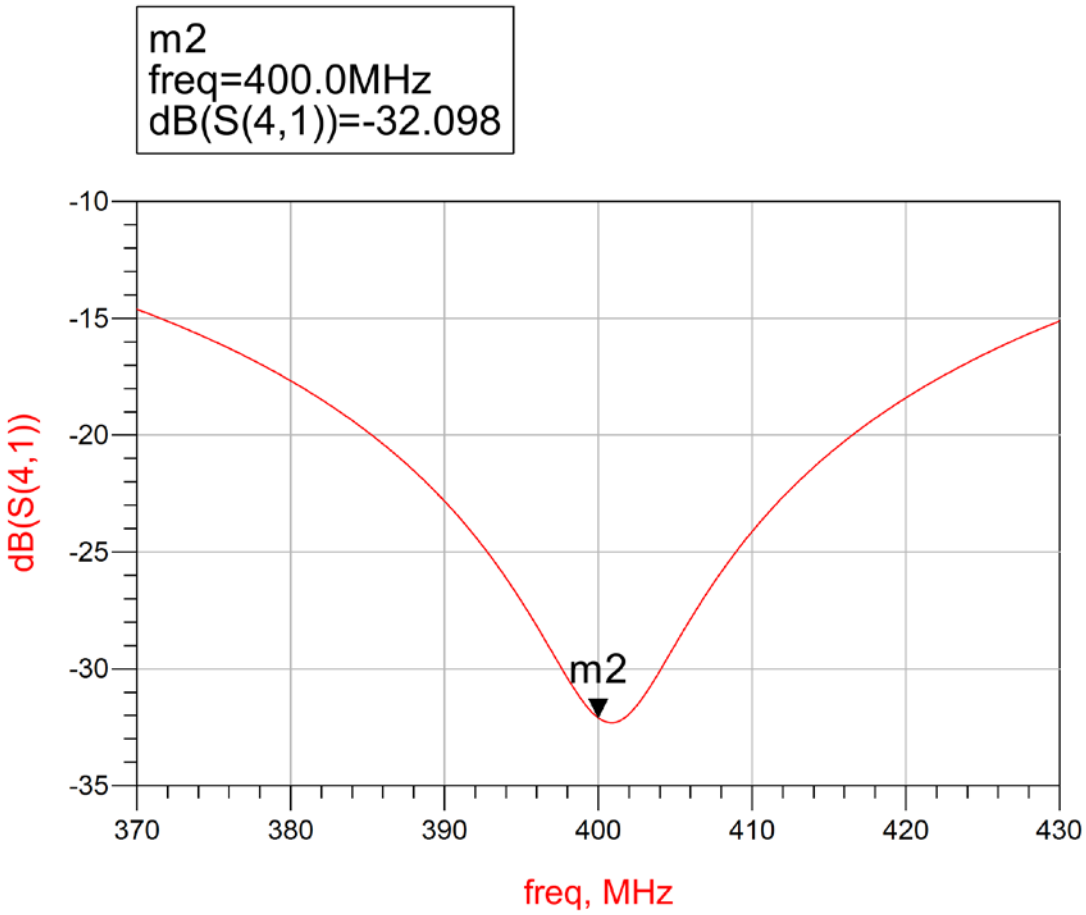

Figure 3.11 Isolation of PORT4

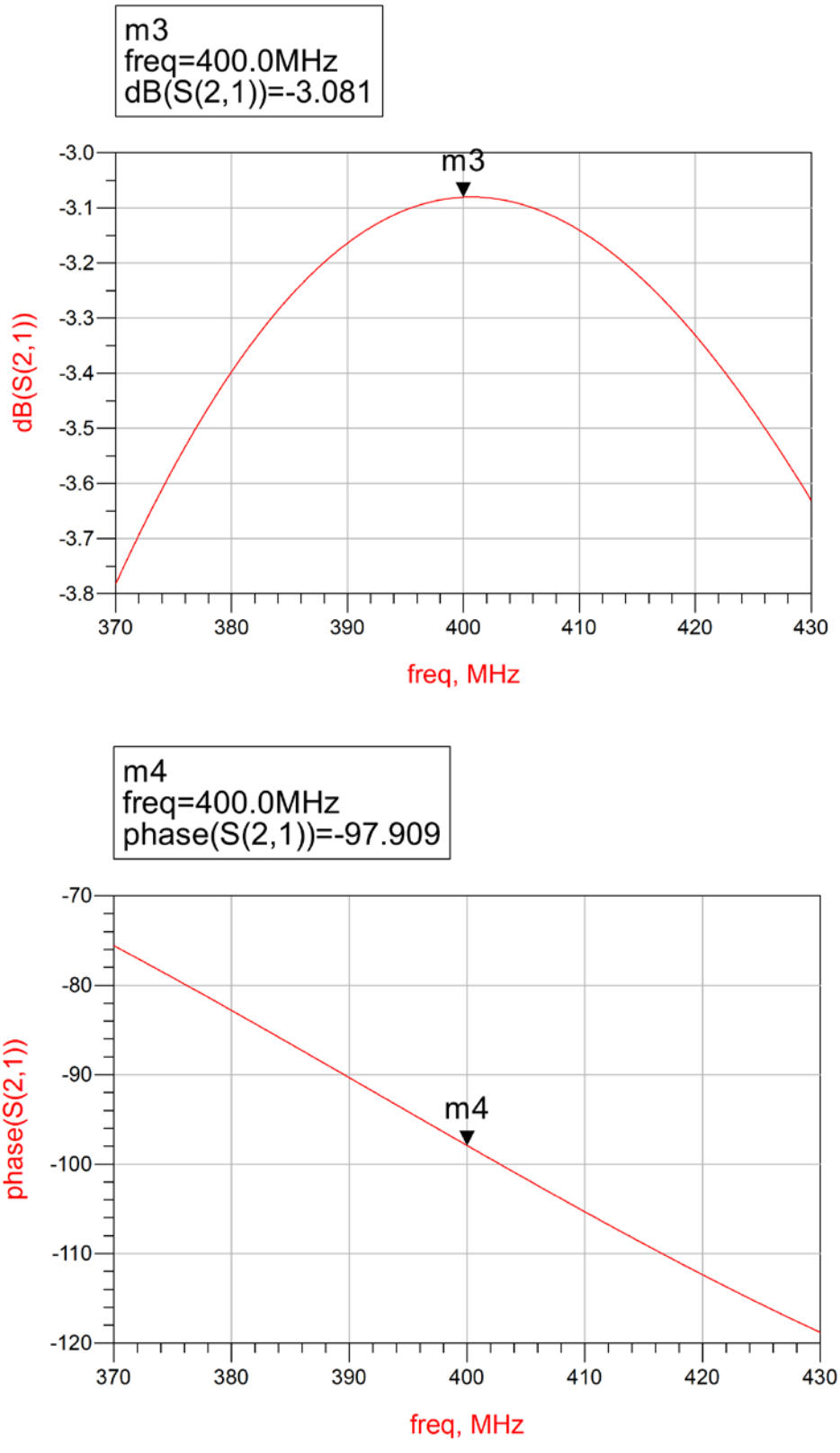

Figure 3.12 Magnitude and Phase for the S21 of PORT2

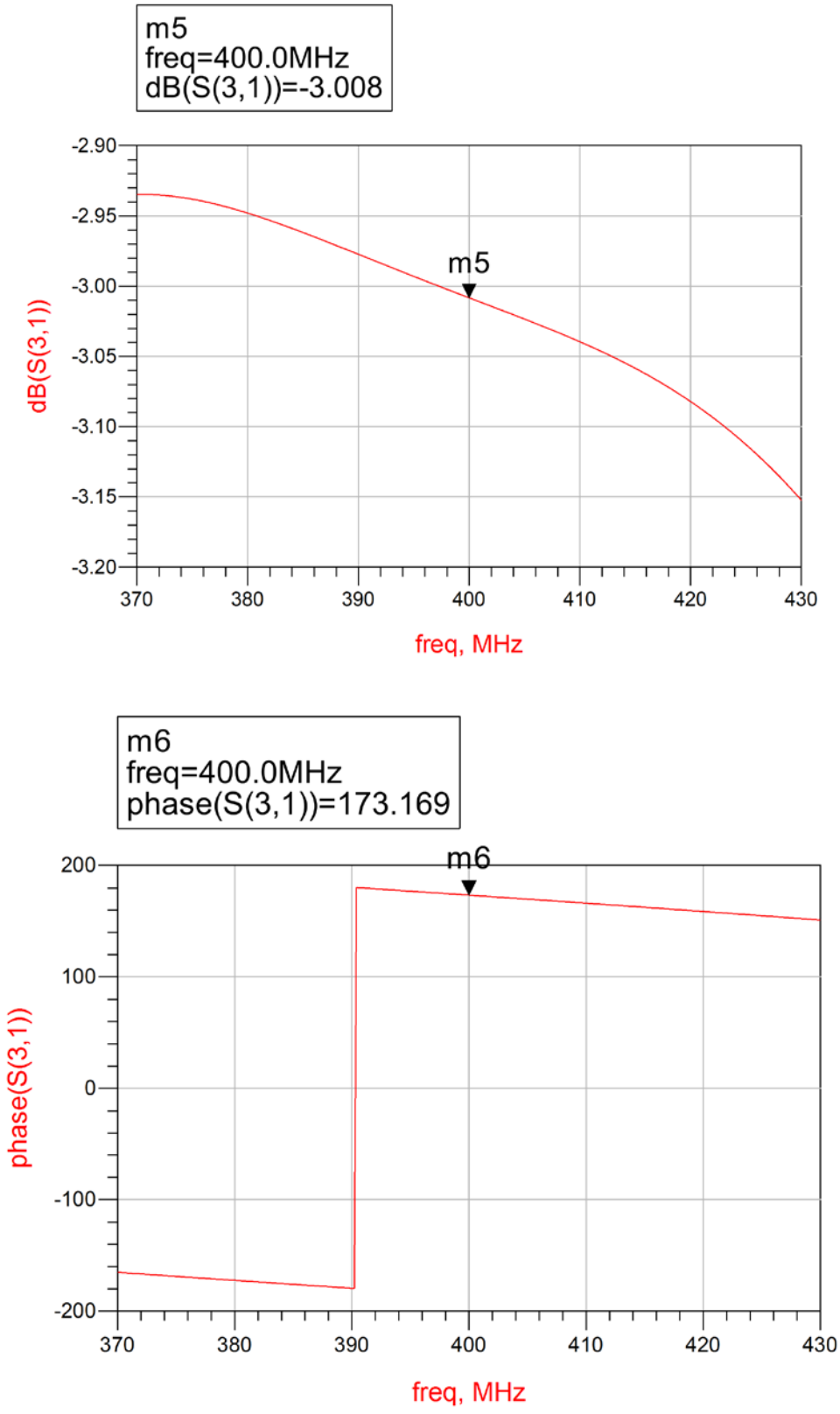

Figure 3.13 Magnitude and Phase for the S21 of PORT3

In the simulation, we got the optimized values:

50ohm(C=8PF,L=18.5Nh)35.4ohm(C=10.5PF,L=13nH)

3.2.3 Bench Test Results

Then we optimized the Quadrature hybrid from the simulation values. And we got the bench test results which correspond very well to the simulation results.

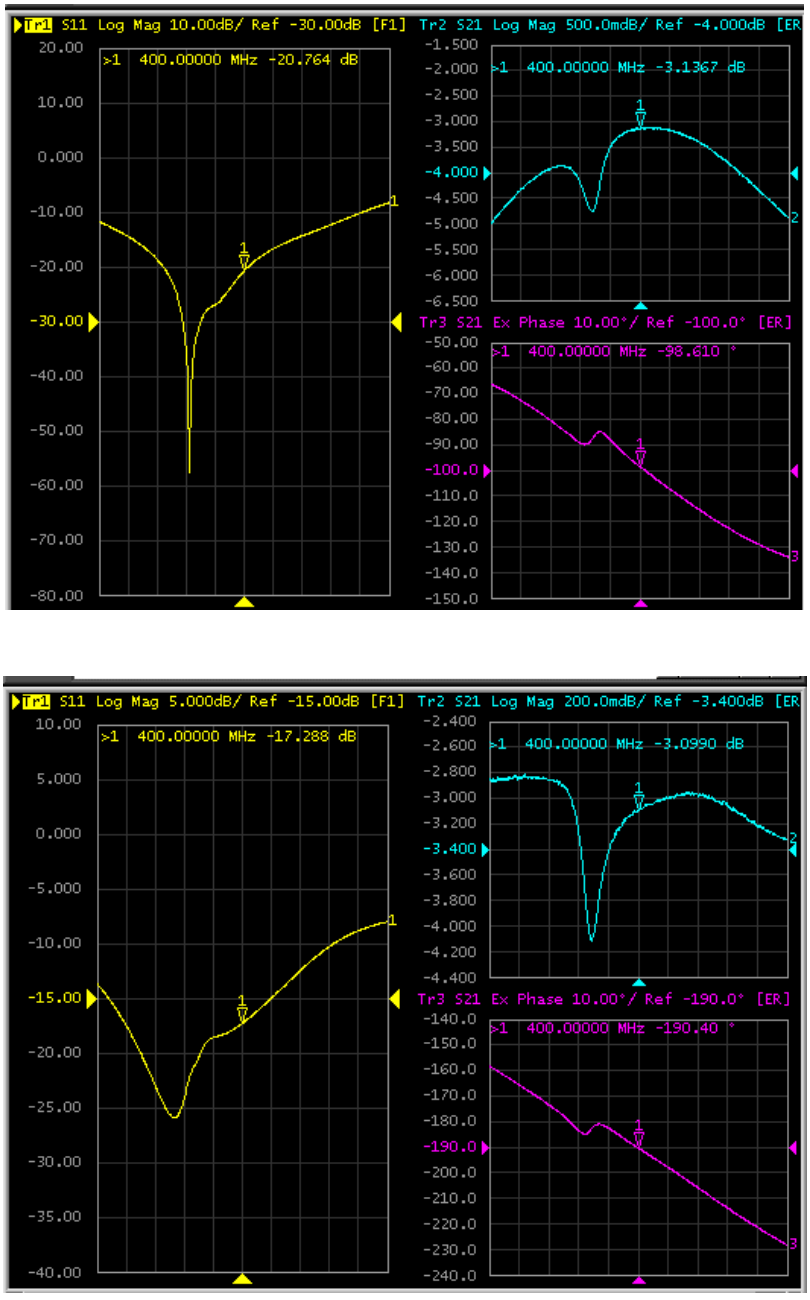

Figure 3.14 Bench test results for PORT1 and PORT2

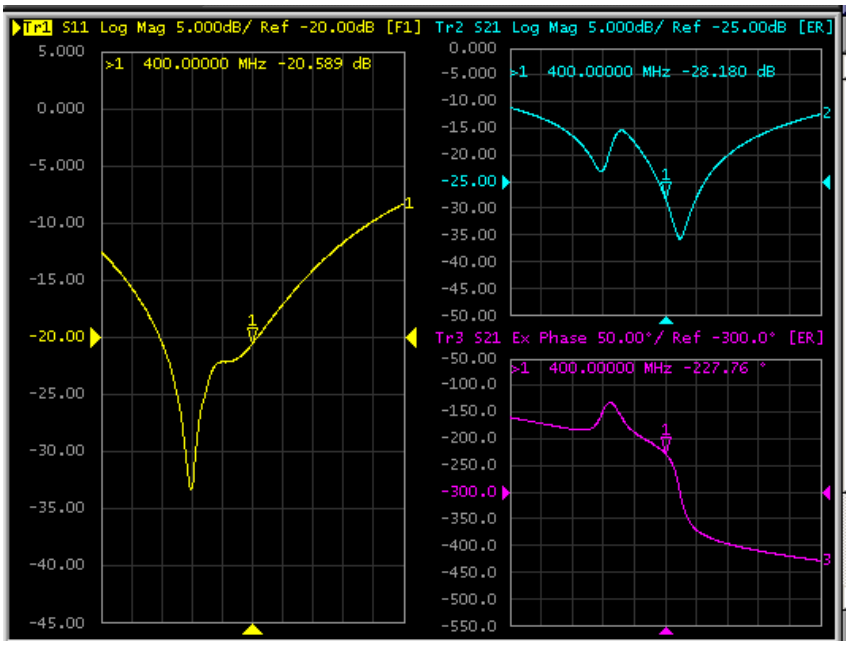

Figure 3.15 Bench test results for PORT4

And the components values are as following:

50ohm(C=9.1PF,L=18.5NH)

35.4ohm(C=6PF,L=18.5NH+164-02Red).

3.3 Low Noise Amplifier (LNA)

3.3.1 Introduction

Signal amplification is one of the most basic and prevalent circuit functions in modern RF and microwave systems. The configuration (Figure 3.16) below shows a general transistor

amplifier circuit. We need to design the input and output matching circuit to determine the impedance matching, stability, gain and noise figure.

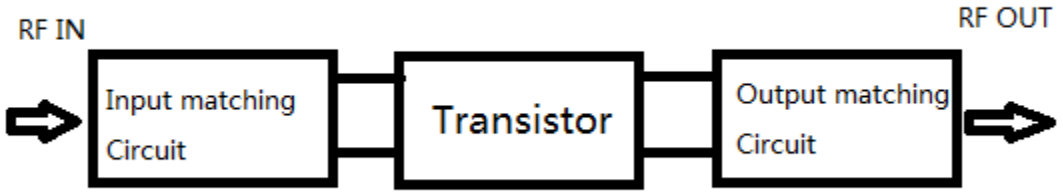

Figure 3.16 A general amplifier schematic

The stability circles can be used to determine regions for Γ_S and Γ_L where the amplifier circuit will be conditionally stable. Also simpler tests can be used to determine unconditional stability. One of these is the K-Δ test, where it can be shown that a device will be unconditionally stable if K>1.

$$K=\frac{1-|S_{11}|^2-|S_{22}|^2+|\Delta|^2}{2|S_{12}S_{21}|}>1$$

With the condition that

$$|\Delta| = |S_{11}S_{22} - S_{12}S_{21}| < 1$$

A very useful gain definition for amplifier design is the transducer power gain, which accounts for both source and load mismatch. We can define separate effective gain factors for the input (source) matching network, the transistor itself, and the output (load) matching network as following:

$$G_S = \frac{1-|\Gamma_S|^2}{|1-\Gamma_{in}\Gamma_S|^2}$$
$$G_0 = |S_{21}|^2$$

$$G_L = \frac{1 - |\Gamma_L|^2}{|1 - S_{22}\Gamma_L|^2}$$

And the overall gain is then $G_T = G_S G_0 G_L$.

Besides stability and gain, the most important design consideration for a low noise amplifier is its noise figure. For a receiver system especially it is often required to have a preamplifier with as low a noise figure as possible because the first stage of a receiver front end has the dominant effect on the noise performance of the overall system. We can use the following equations to determine.

$$\mathrm{F} = F_{min} + \frac{R_N}{G_S}\left|Y_S - Y_{opt}\right|^2$$

Here, Y_S means source admittance presented to transistor, Y_{opt} means optimum source admittance that results in minimum noise figure, F_{min} means minimum noise figure of transistor, R_N means equivalent noise resistance of transistor, G_s means real part of source admittance.

3.3.2 Design and Simulation

For this LNA on the front end circuit, we chose one-stage. Because there is amplifier installed in the Bruker 9.4 T scanner system. And if the gain is too high, the system will block the RF signal from the coil. The transistor we chose here is ATF-54143 FET. And an active biasing design is applied here for the DC bias. For the reason that it can provide a very stable working point with large temperature variations. The bias circuit was built with PNP and resistor network. The circuit diagram is shown as following. We need to check the data sheet of the PNP

transistor to I-V curve and figure out the DC current and gain. Then we can calculate the values of the resistors according to the basic characteristics of the transistors.

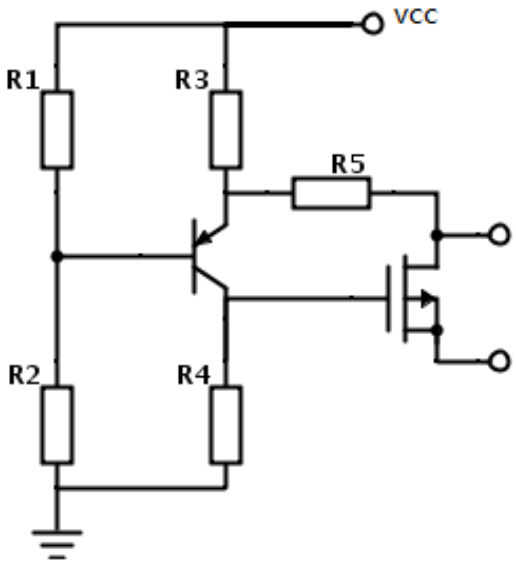

Figure 3.17 DC bias Schematic

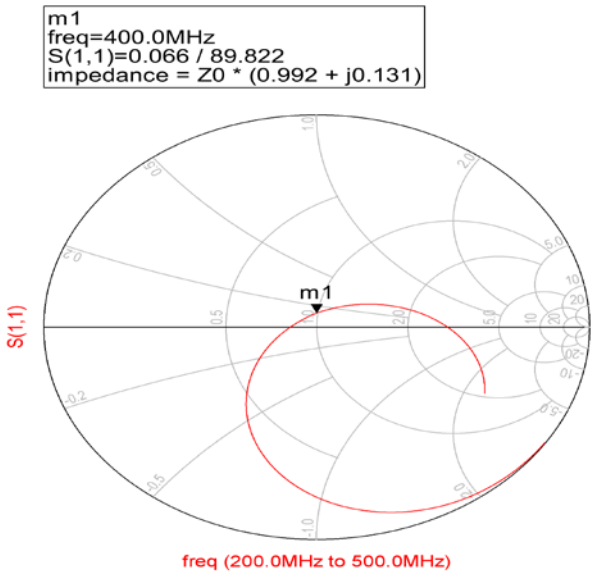

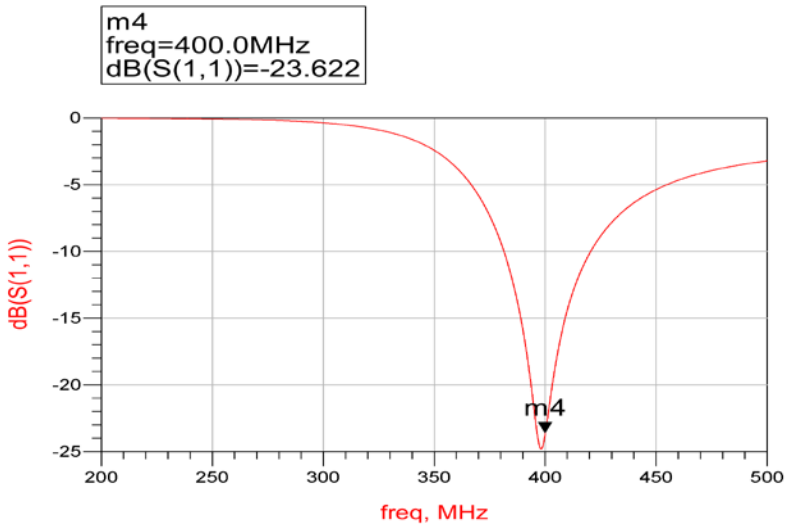

Figure 3.18 Input Impedance of the LNA

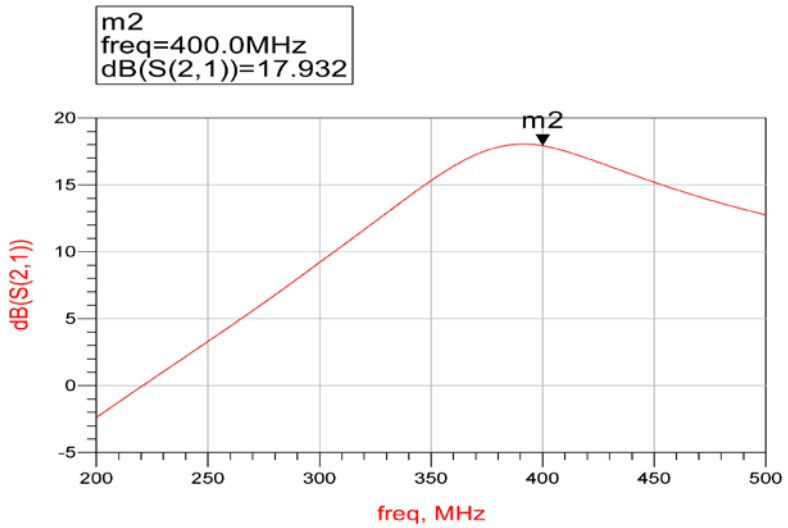

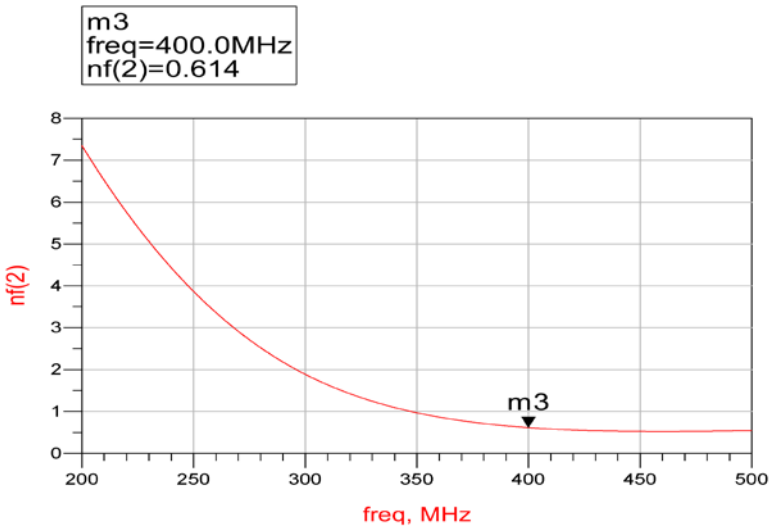

Figure 3.19 Gain and Noise Figure

3.3.3 Bench Test Results

There are three parameters we need to confirm the design and fabrication, input impedance, gain and noise figure. We use Network Analysis to measure the input impedance and Noise Analysis to measure the gain and noise figure. The results are shown below (Figure 3.20). We can see from the bench test results that that the gain is a little bit lower than the simulation value. In my point the reason maybe that we use a trimmer inductor for the input impedance matching, the Q of which is not very high. And the noise figure cannot be measured exactly under our test environment, but it does not matter for the performance according to our previous experience.

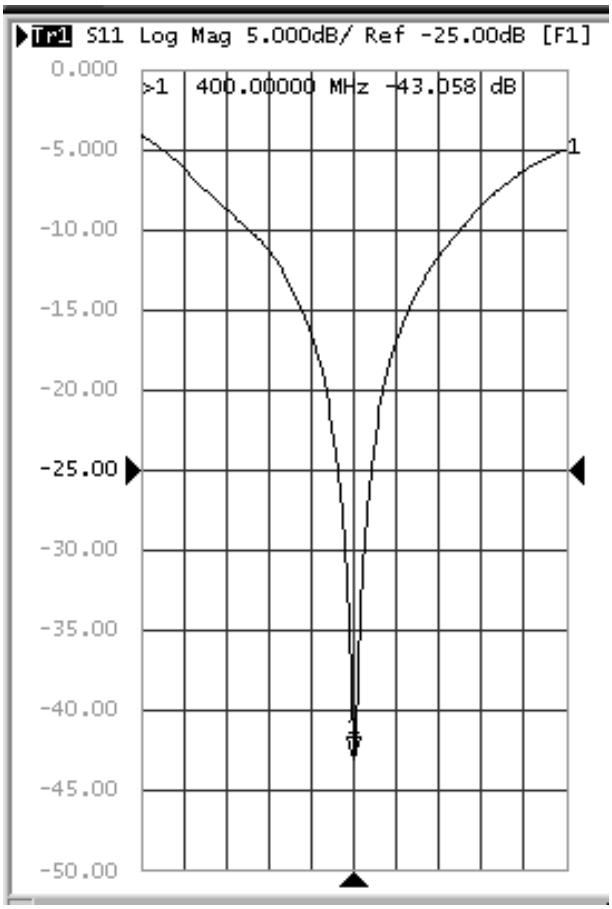

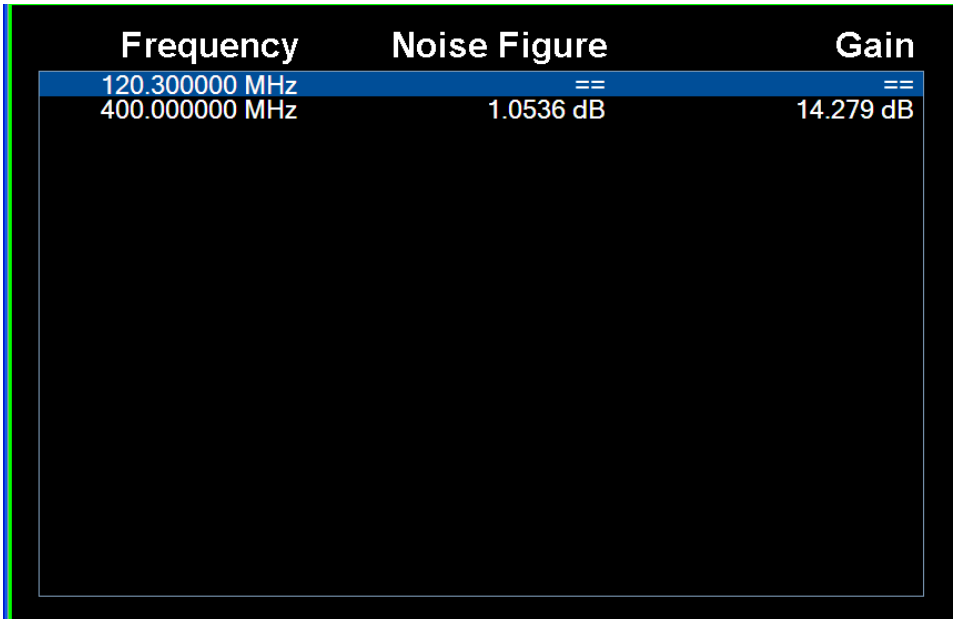

Figure 3.20 Bench test of the LNA

Chapter 4 Coil Fabrication and Scanner Results

The birdcage coil was fabricated on the housing frame printed by 3D printer with AWG#16 copper wires. And according to the theory of high-pass birdcage coil, the capacitors were placed on the rings uniformly and no capacitors were placed on the legs. Also, we used three capacitors instead of one capacitor on one ring. There are two reasons why we did that. First, in high magnetic field, the capacitor and the subject may be coupled if the value of the capacitor is too small. Second, using three capacitors instead of only one, we can reduce the transmit RF voltage on the capacitors which can protect the capacitors and make the coil robust.

4.1 Coil Housing Design and Fabrication

There are totally three parts of the coil housing frame. One is an acrylic tube bought online. And we designed the other two parts in the software AutoCAD and then printed by 3D printer.

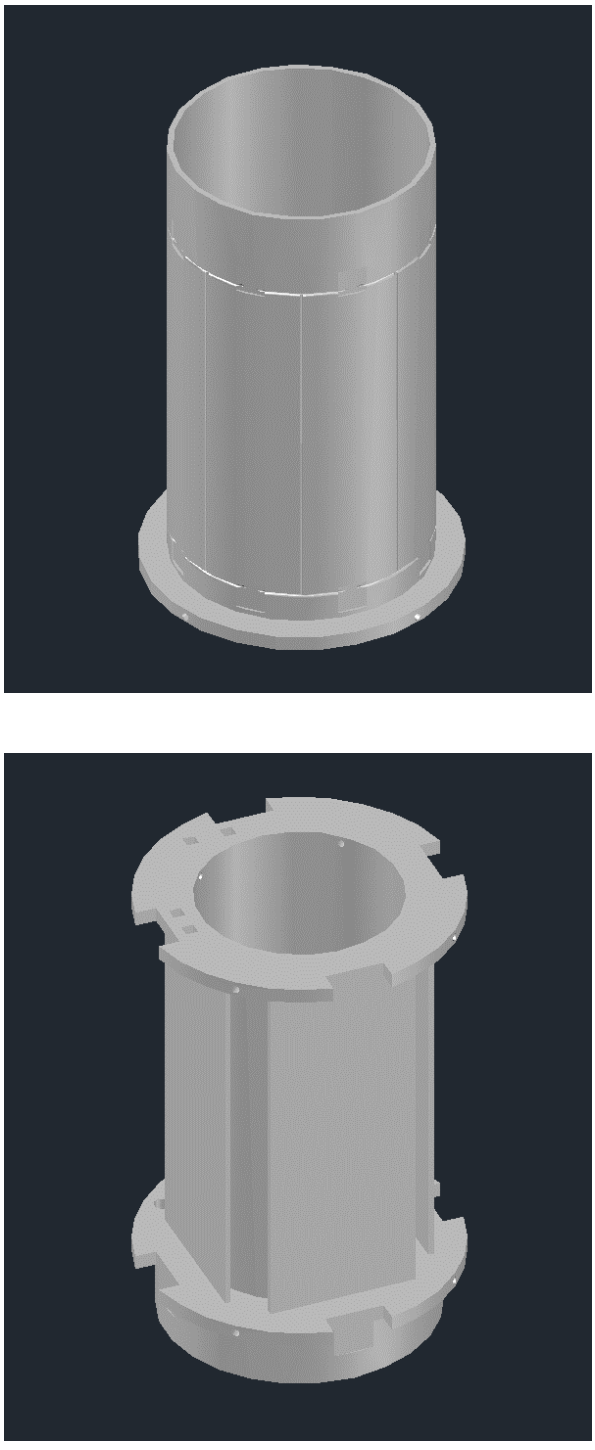

Figure 4.1 Coil Housing Design in AutoCAD

The coil housing frame shown in Figure 4.1(the upper one) is the part for coil. The grooves are for the copper wires fasten. And we can see that the patches for the capacitors are large enough for three capacitors in series. The coil housing frame shown in Figure 4.1(the under one) is the part for the front-end circuits. And we have designed holes for the cable connection.

Figure 4.2 Coil Housing Frame Printed out by 3D printer

The coil is fabricated as shown in the figure 4.2. And the shield was fabricated on the tube. We pasted four copper tapes on the tube, and soldered five 1nF capacitors between two adjacent tapes. And the capacitors were used here to prevent the image effect for function MRI.

4.2 Tuning, Matching and Decoupling of the Coil and Bench test results

The capacitors we used for the coil is 7PF. And the first step is tuning. According to the birdcage theory, there should be N/2+1 peaks we can see. Here N=8, so totally five distinct resonant modes. And the dominant birdcage mode is at the second highest frequency. The way for tuning is that we tune the capacitors which are opposite to the exciting ports to tune the resonant frequency of the desired mode to 400Mhz. That is because the current through the capacitors which are on the opposite of the exciting ports is the strongest which means that tuning these capacitors can tune the resonant mode distinctly. The tuning capacitors we used here are 2.7PF.

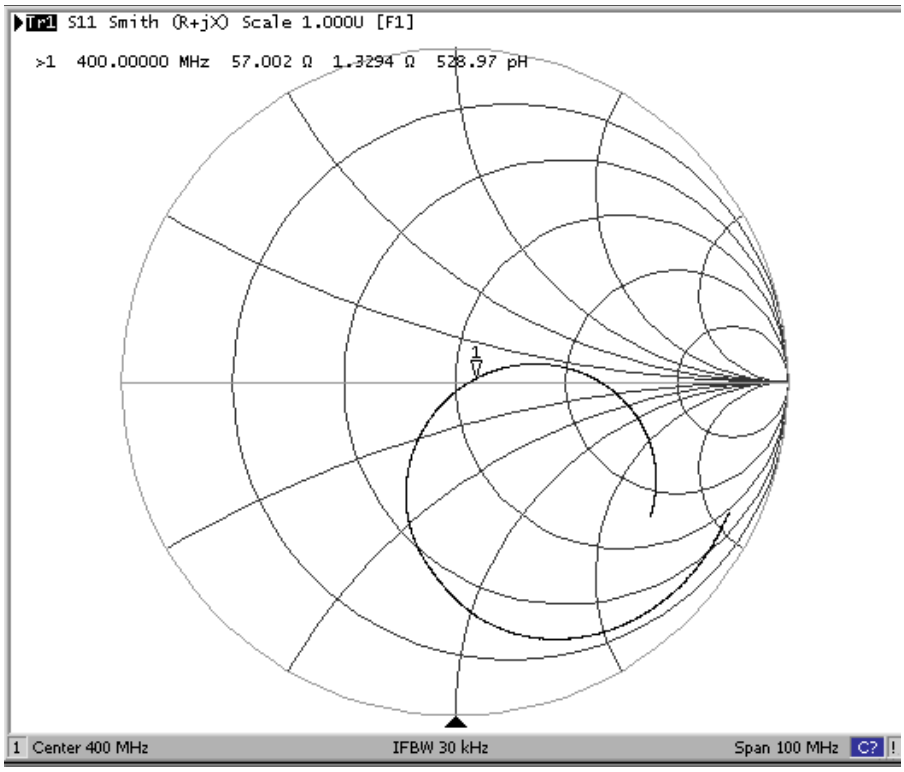

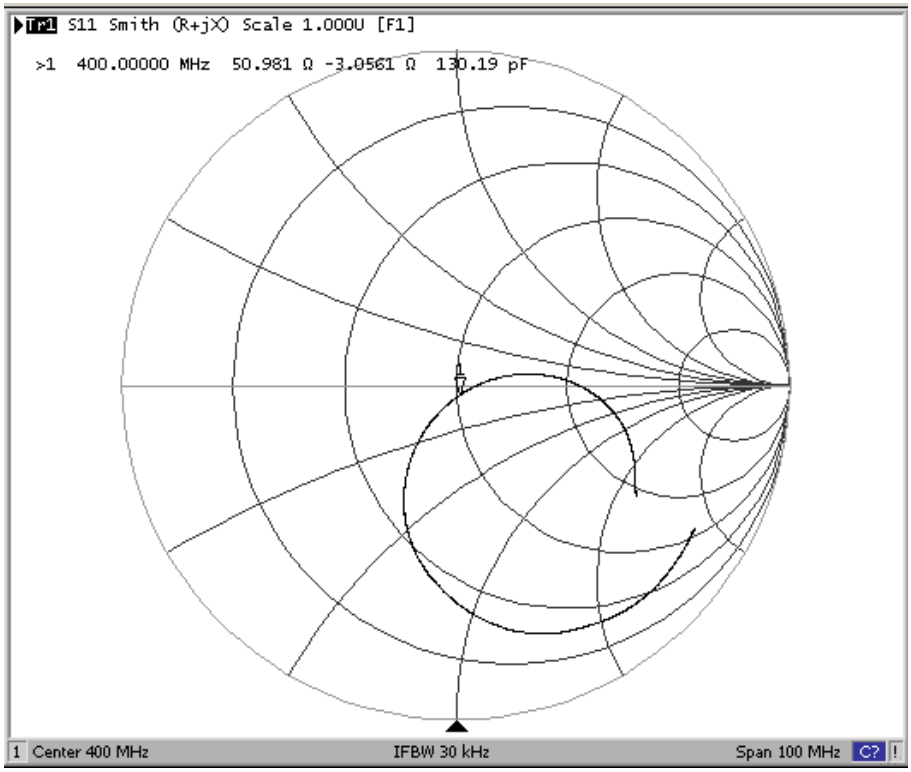

Figure 4.3 Impedance of the coil measured from PORT1 and PORT2

We can see from the figure 4.3 above that we have tune the coil to a pure real part for the resistance. If the coil is inductive or capacitive, the capacitors may store energy during the scanning which may make them broken.

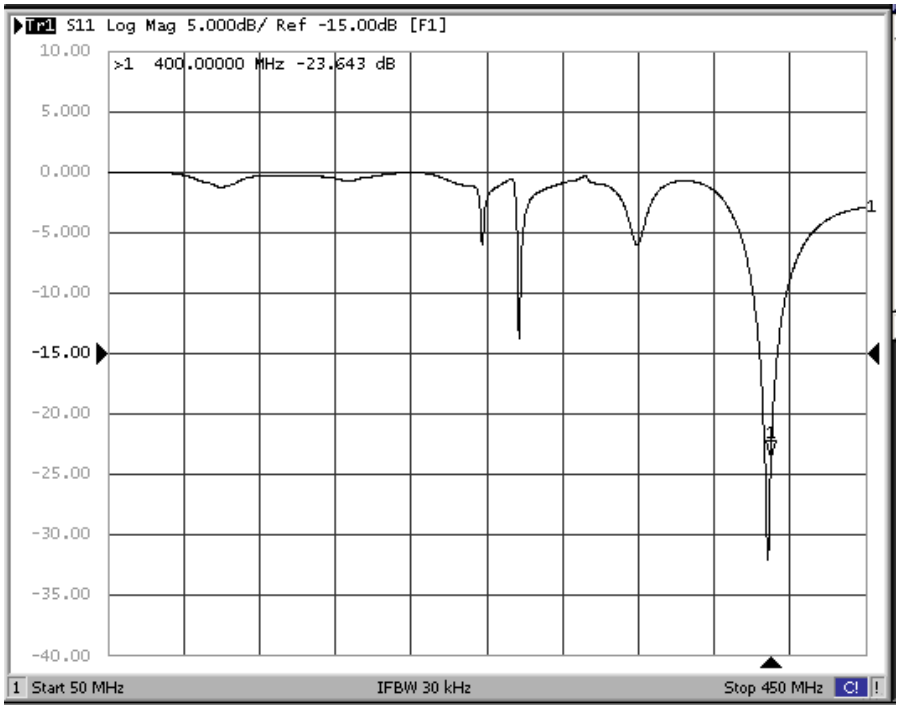

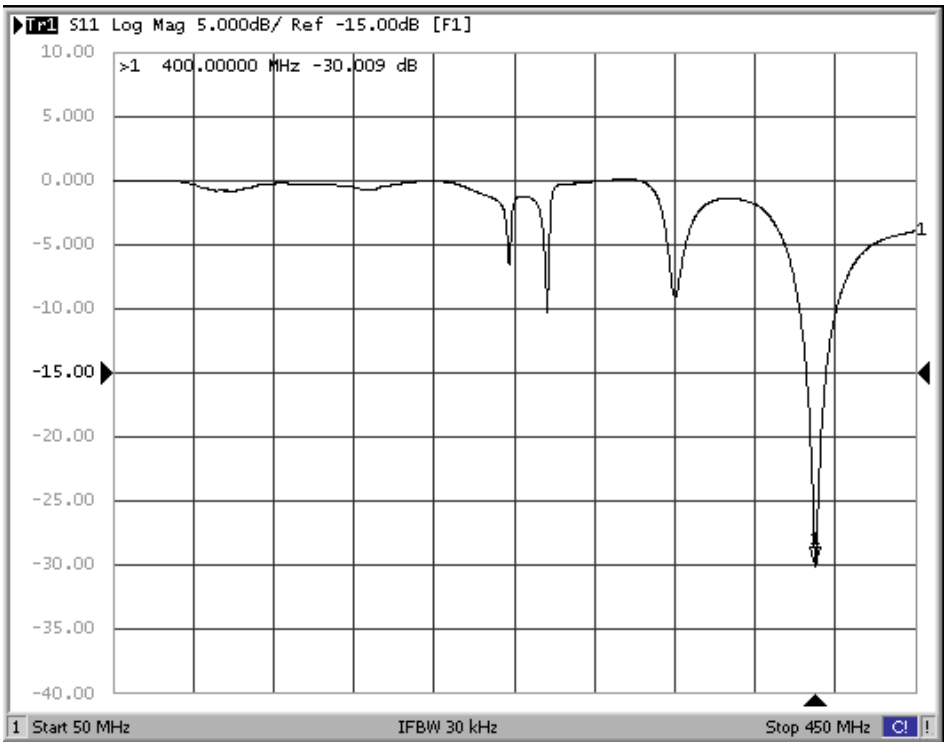

Figure 4.4 S11 measured from PORT1 and PORT2 in a large frequency span

The figure 4.4 above shows four distinct resonant modes counting from low frequency. And the bench test results are comparable to the simulation results. That is one way we check the resonant mode is right or not. And usually we use another way for double check. Connect Port 1 of the network analysis to excite the coil and connect Port 2 of the network analysis to a probe to detect the field distribution generated by the coil. If we have got the right mode, we can see the S21 measured by the probe should be around -25dB in the area of interest (Figure 4.5).

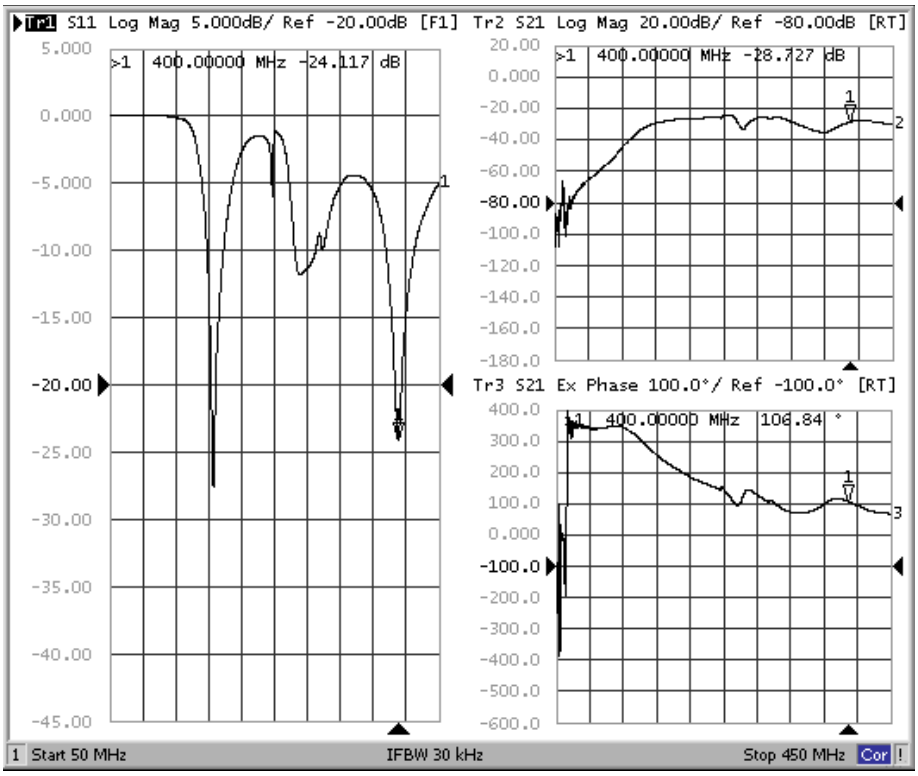

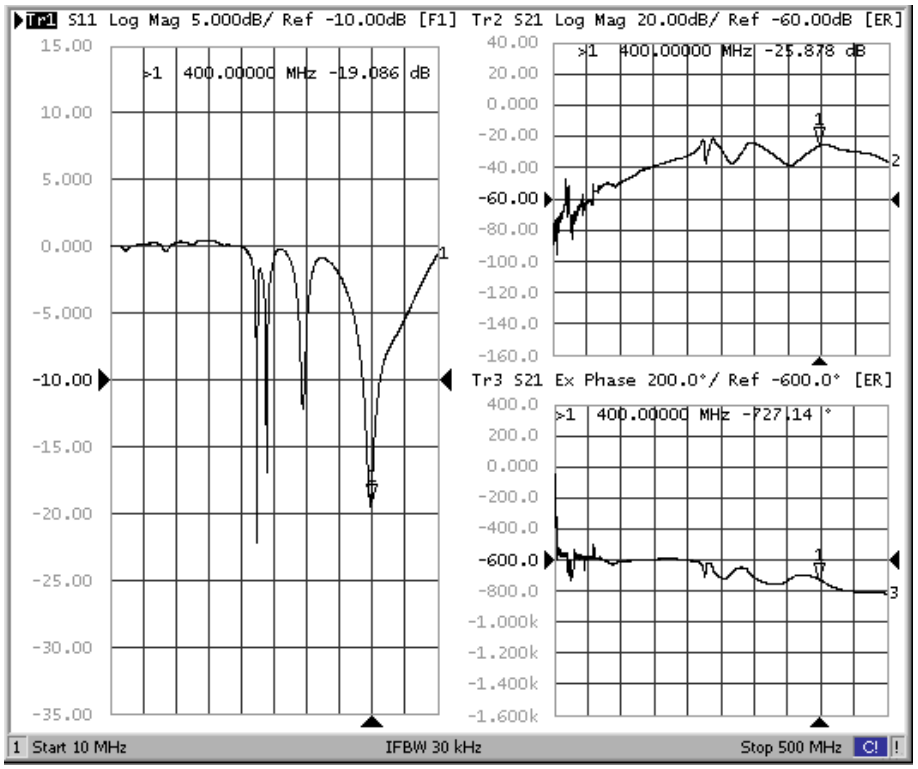

Figure 4.5 Field Distribution measured from PORT1 and PORT2

After tuning the coil to the right mode, we should match the coil to impedance of the system, 50ohm. Though the impedance of the coil is around 50ohm after tuning, and the S11 is good enough, we should still match the coil. Because the Q of the coil without matching board is not very high. And we have tested a similar coil without matching at 7T, the scanning results of which is not good. So here we used a symmetrical L-network to match the coil. And usually there will be coupling problem between the two ports. Fortunately, the coupling of this coil is not serious. S21 is around -18dB. But if meeting the coupling problem, we can tune the capacitor between the two exciting ports to minimize the S21. The figure 4.6 shown below is measured when connecting one port to PORT1 of the network analysis and another port to PORT2 of the network analysis.

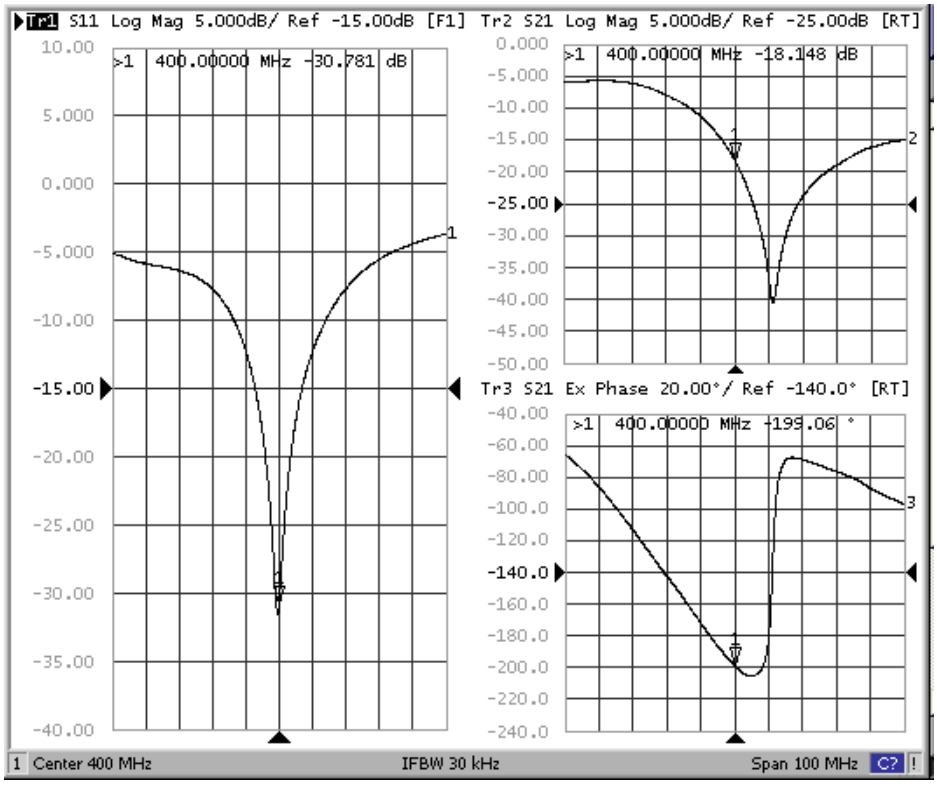

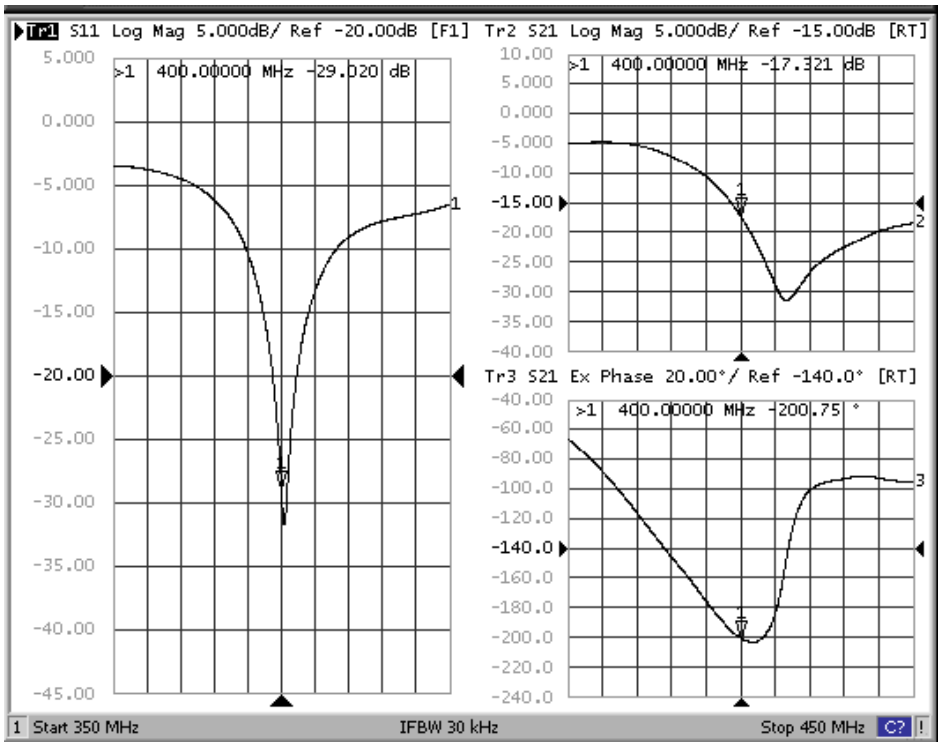

Figure 4.6 S11 and S21 measured from PORT1 and PORT2

4.3 Coil Connection to the System and Scanning Results

There are totally four cables connecting the coil to the scanner system. 1) TX cable connected to TX cable of the scanner system. 2) TX DC cable connected to the act.dec port of the scanner system. 3) RX cable connected to the RX port of the interface box on the ground. 4) RX DC cable connected to the DC supply outside the scanning room.

Figure 4.7 The completed coil system

The figure 4.7 shows how the coil finally looks like. And we used BNC, SMA, Type-N for the connection. When testing a coil, we will not usually test a real subject first. Instead, making a phantom to replace the mouse. The test subject is a bottle, the size of which is similar to the mouse for animal research according to the request from UAB. And we fill the bottle with saline water, the density of which is 3.95g/L (Figure 4.8). By this way, we can make the phantom as closely as to a real mouse.

Figure 4.8 Phantom used for the scan

The first step for scanning was to apply a gradient echo sequence to scan. And we can get the images of three planes, transverse, sagittal and coronal for checking the coil works or not. The second step was to apply a spin echo sequence to scan, which is widely used for mouse imaging. And the last step is to measure the SNR as a reference.

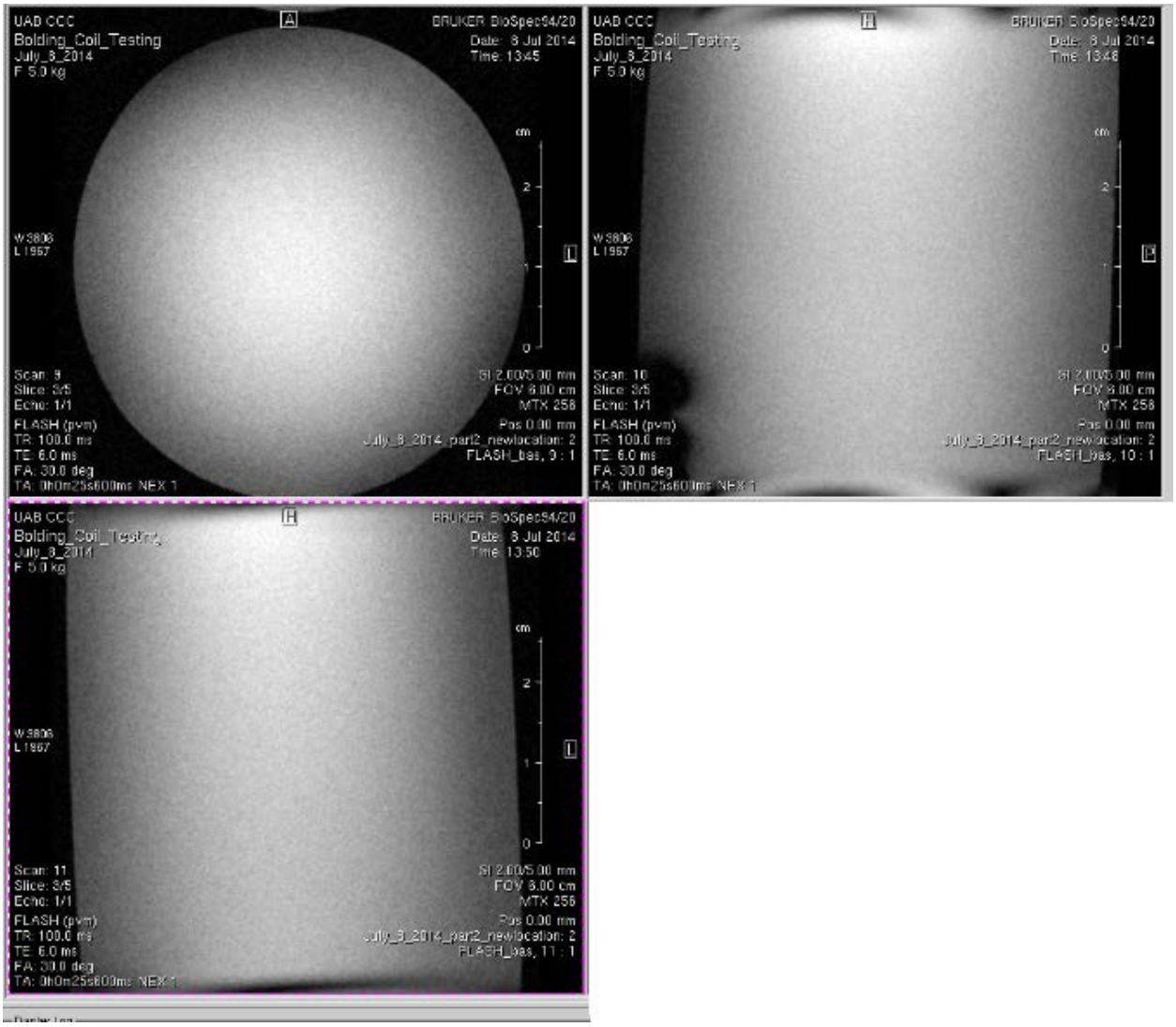

Figure 4.9 Images from three planes, Transverse, Sagittal, Coronal

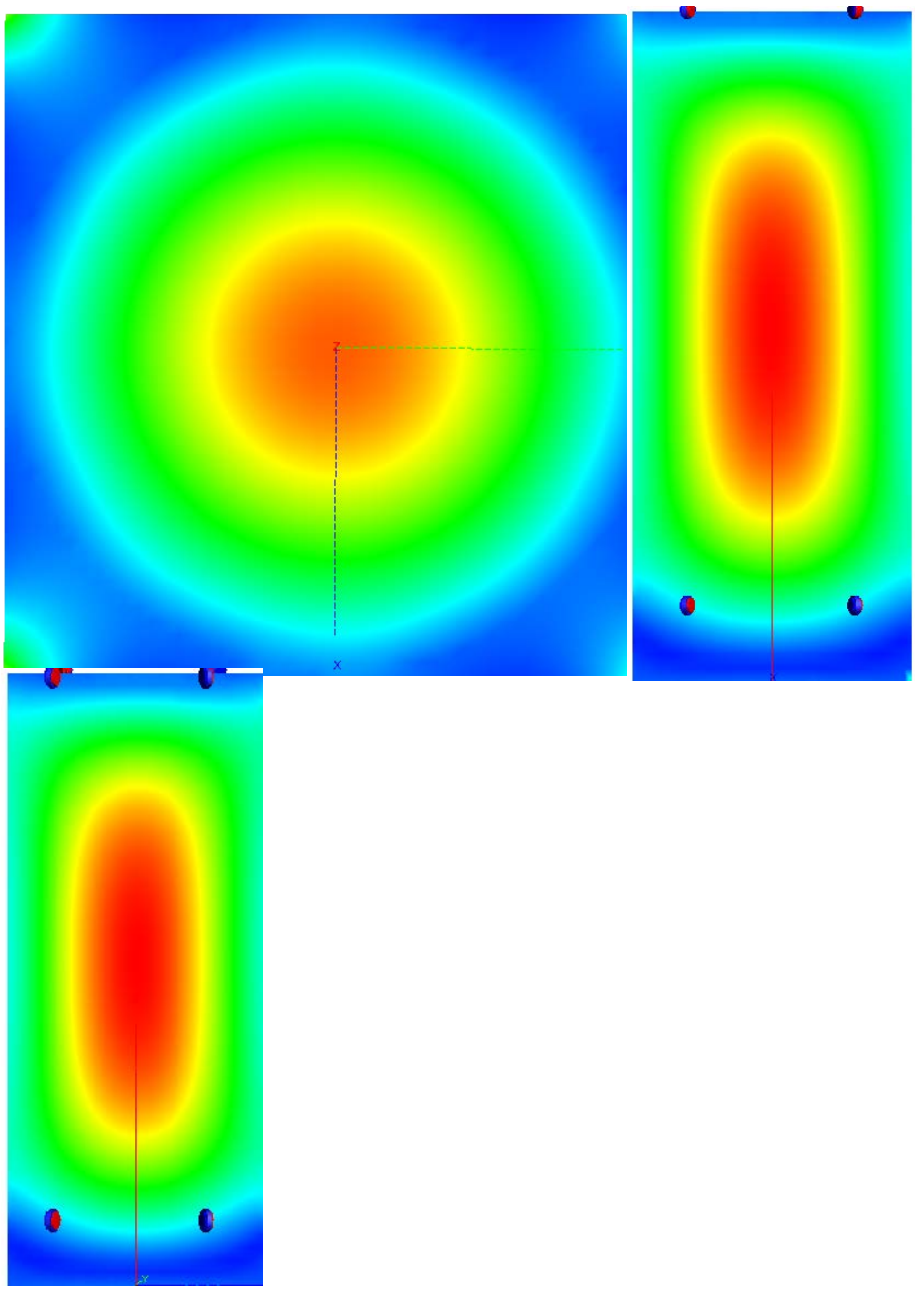

Figure 4.10 Comparison with the simulation results

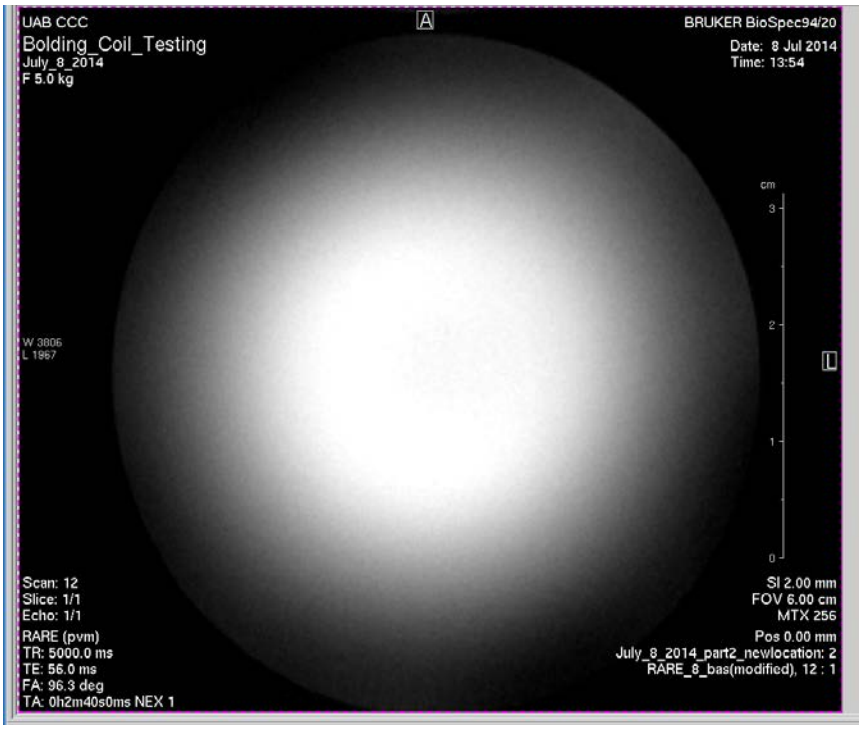

Figure 4.11 Image when applying spin echo

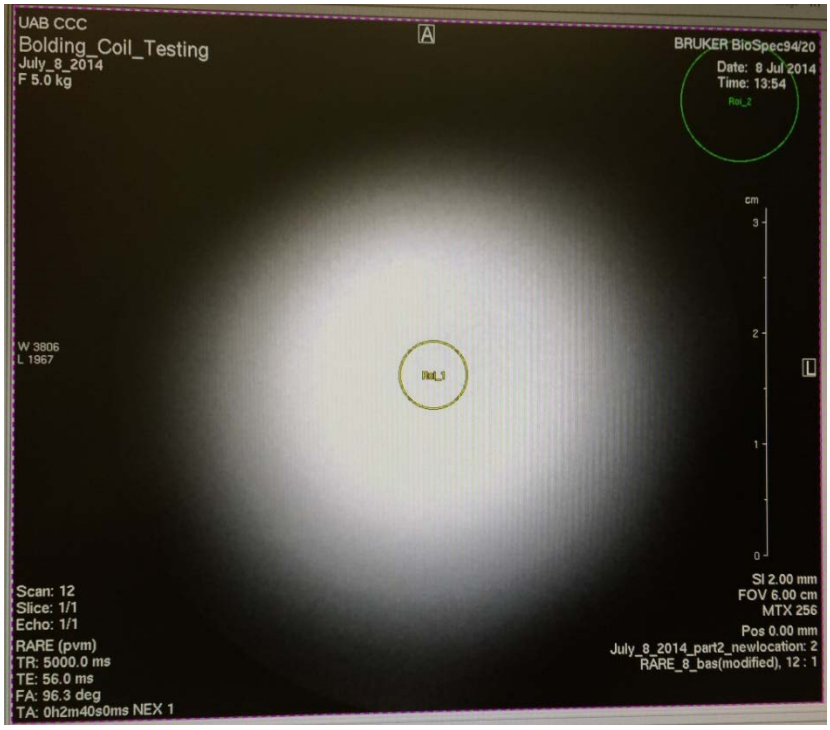

Figure 4.12 SNR

The parameters for the gradient echo sequence are as following. TR=100ms, TE=6.0ms, FOV=6cm, MATRIX=256. And the parameters for the spin echo sequence are as following. TR=5000ms, TE=56ms, FOV=6cm, MATRIX=256. We selected a certain area in the center of the phantom to get the signal level, and selected a certain area in the background to get the noise level (Figure 4.12). We can read the data from the software. The signal is 239 and noise is 1.57, so the SNR is 239/1.57=152.2. We can use this SNR value as a reference comparable to other coils for this system.

Chapter 5 Discussion and Future Work

In this thesis, a basic concept of a Quadrature MRI Birdcage coil and a brief procedure of fabrication are introduced. The coil was designed and simulated in the software FEKO. And then we designed the housing frame in the AutoCAD and print it out by 3D printer. After tuning the coil to 400Mhz (9.4T), designing and fabricating the front end circuit board, we assembled the coil and connected it to the scanner system for testing.

From the scanning results, we can see that in a certain center area, the image is very homogenous and no artifact is detected with a high SNR achieved. And images from three planes correspond very well to the profile and simulation results. So we can say here, the coil is up to standard.

5.1 Birdcage Coil Fabrication Issues

The following is a list of issues about coil design and fabrication that I have faced during my work. For the next coil that I will build, I should consider these factors into my design.

Images are good only in a certain center area of the subject. This problem is limited by the profile of birdcage coil. So we can build a surface phased-array coil instead to solve this issue. But we should care more about the symmetry of a surface coil especially when the number of channels is 4 or more.

The performance of the front end circuit can be improved. We can see from the bench test of the T/R switch that the loss for both TX and RX conduction is a little bit high. And if we can reduce the loss, we can get a high SNR and a better transmit efficiency. Another one is for

the Quadrature hybrid. The isolation for the PORT 4 is not good enough, which means that the signal combine is not very good.

As the birdcage coil is fixed tuned, if we change a subject whose size is much smaller, the birdcage coil may be totally detuned and does not work anymore. So one way to solve this problem is that we can replace the capacitors on the tuning position with trimmer capacitors. And add some tools for the housing design so we can retune the coil when different subjects are in it. However, there may be new problems emerge, such as the trimmer capacitors cannot resist a high voltage which may be applied in some sequence.

5.2 Future Work

We are now designing and fabricating a 4-channel Transmit and Receive surface phased-array coil for the 9.4T scanner (Figure 5.1). We can see the overlap decouple between the adjacent channels. And we attempt to design a more complicated front end circuit to get two modes of the image. We hope we can improve the SNR and get a more homogenous image by this coil compared with the birdcage coil.

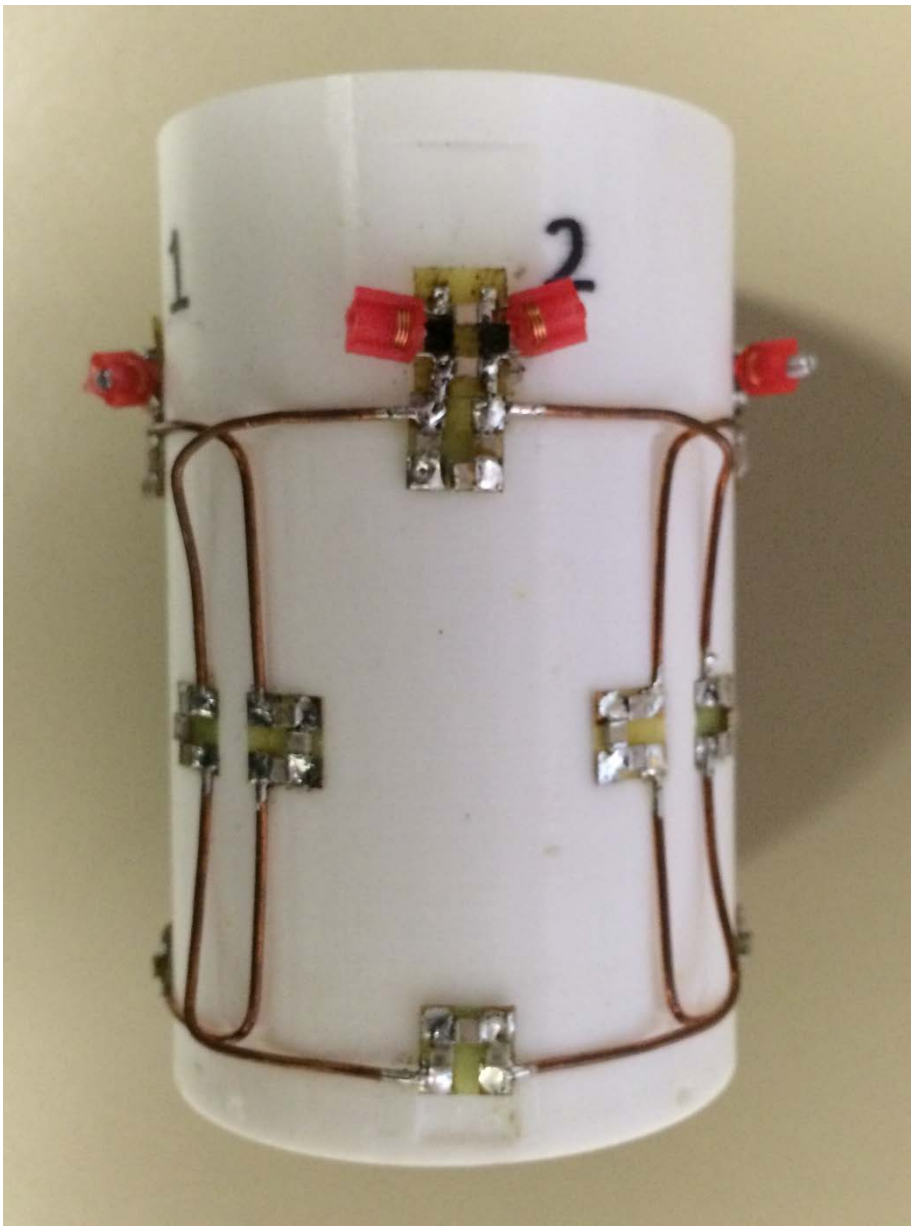

Figure 5.1 4chan coil for 9.4T

References

[1] J.M. Jin, “Electromagnetic Analysis and design in Magnetic Resonance Imaging”, Boca Raton, FL, CRC Press, 1988, ISBN – 13 978-0849396939.

[2] “A High-Pass Detunable Quadrature Birdcage Coil at High-Field”, (May 2008). Vishal VirendraKampani, B.S., University of Illinois-Urbana Champaign.

[3] “Microwave Engineering”, David M. Pozar, November 22, 2011, ISBN-13: 978-0470631553.

[4] “A High Power Solid State T-R Switch” by Gerald Hiller and Rick Cory, Skyworks Solutions, Inc.

[5] “The Quadrature Hybrid Coupler”, Jim Stiles, the University of Kansas. 4/17/2009.

[6] “Low-Noise Amplifier Design and Optimization”, Marcus Edwall, Luleå University of Technology.

[7] “Microwave Transistor Amplifiers: Analysis and Design”, Guillermo Gonzalez, August 30, 1996, ISBN-13: 978-0132543354.

[8] “A 3 Tesla High-Pass Transmit and Receive Quadrature Birdcage Coil For Animal Imaging”, Sep 2012, Xiaotong Sun, Auburn University.

[9] Catherine Westbrook, et al**, “**MRI in Practice”, June 30, 2005, ISBN-13: 978-1405127875.

[10] “Applied Electromagnetics: Early Transmission Lines Approach”, Stuart M. Wentworth, Auburn University, January 9, 2007**,** ISBN-13: 978-0470042571.

[11] Doty FD, Entzminger G, Hauck CD, Staab JP.1999. Practical aspects of birdcage coils. J Magn Reson 138(1) :144-54.

[12] Ibrahim TS, Lee R, Baertlein BA, Kangarlu A, Robitaille PL.2000. Application of finite difference time domain method for the design of birdcage RF head coils using multi-port excitations. Magn Reson Imaging 18(6):733-42.

[13] “A 4.7 Tesla 4-Channel Transmit and Receive MRI Quadrature Birdcage Coil Design and Fabrication for Monkey Head Imaging”, Aug 2013, Xiaotong Sun, Auburn University.

[14] Jin J.1998. Electromagnetic analysis and design in magnetic resonance imaging.Florida:CRC Press.

[15] Wichern AHW, Leussler CG.1991. MR examination apparatus comprising a circuit for decoupling the two coil systems of a quadrature coil arrangement. U.S patent 4 998 066.

[16] “Advanced Parallel Magnetic ResonanceImaging Methods with Applications to MR Spectroscopic Imaging”, RicardoOtazo, University of New Mexico, USA, 2006.

[17] S. Wang et al., B1 Homogenization in MRI, IEEE Trans. Medical Imaging, vol. 28, no. 4, pp. 551-554, 2009.

[18] A. Kumar and P.A. Bottomley, Optimized Quadrature Surface Coil Designs, Magn. Reson. Mater. Phy., vol. 21, no. 1-2, pp. 41-52, March 2008.

[19] IEC 60601-2-33, Ed. 2.0, Medical Electrical Equipment, Part 2-33, Particular requirements for the safety of magnetic resonance equipment for medical diagnosis, 2002.

[20] J.P. Hornak, The Basics of MRI, 2011

[21] Huettel, S.A. Functional Magnetic Resonance Imaging. USA: Sinauer. p. 31.

[22] Vaughan, J.T.; Adriany, G.; Snyder, C.J.; Tian, J.; Thiel, T.; Bolinger, L.; Liu, H.; DelaBarre, L.; Ugurbil, K. (1 October 2004). "Efficient high-frequency body coil for high-field MRI". Magnetic Resonance in Medicine 52 (4): 851–859.